

Data Fusion for Integrative Species Identification Using Deep Learning

LARA M KÖSTERS¹, KEVIN KARBSTEIN¹, MARTIN HOFMANN², LADISLAV HODAC¹, PATRICK MÄDER^{2,3,4}, AND JANA WÄLDCHEN³

Biogeochemical Integration, Max-Planck-Institute for Biogeochemistry, Jena, 07745, Germany

² Data-intensive Systems and Visualization Group (dAISY), Technical University Ilmenau, Ilmenau, 98693, Germany

³ German Centre for Integrative Biodiversity Research (iDiv) Halle-Jena-Leipzig, 04103, Leipzig, Germany

⁴ Faculty of Biological Sciences, Friedrich Schiller University Jena, Jena, 07745, Germany

**Mail: lkoesters@bgc-jena.mpg.de, orcid: 0000-0002-7913-2377*

ABSTRACT

1 DNA analyses have revolutionized species identification and taxonomic work. Yet,
2 persistent challenges arise from little differentiation among species and considerable
3 variation within species, particularly among closely related groups. While images are
4 commonly used as an alternative modality for automated identification tasks, their
5 usability is limited by the same concerns. An integrative strategy, fusing molecular and
6 image data through machine learning, holds significant promise for fine-grained species
7 identification. However, a systematic overview and rigorous statistical testing concerning
8 molecular and image preprocessing and fusion techniques, including practical advice for
9 biologists, are missing so far. We introduce a machine learning scheme that integrates both
10 molecular and image data for species identification. Initially, we systematically assess and
11 compare three different DNA arrangements (aligned, unaligned, SNP-reduced) and two
12 encoding methods (fractional, ordinal). Later, artificial neural networks are used to extract
13 visual and molecular features, and we propose strategies for fusing this information.
14 Specifically, we investigate three strategies: I) fusing directly after feature extraction, II)
15 fusing features that passed through a fully connected layer after feature extraction, and

16 III) fusing the output scores of both unimodal models. We systematically and statistically
17 evaluate these strategies for four eukaryotic datasets, including two plant (Asteraceae,
18 Poaceae) and two animal families (Lycaenidae, Coccinellidae) using Leave-One-Out
19 Cross-Validation (LOOCV). In addition, we developed an approach to understand
20 molecular- and image-specific identification failure. Aligned sequences with nucleotides
21 encoded as decimal number vectors achieved the highest identification accuracy among
22 DNA data preprocessing techniques in all four datasets. Fusing molecular and visual
23 features directly after feature extraction yielded the best results for three out of four
24 datasets (52-99%). Overall, combining DNA with image data significantly increased
25 accuracy in three out of four datasets, with plant datasets showing the most substantial
26 improvement (Asteraceae: +19%, Poaceae: +13.6%). Even for Lycaenidae with high
27 identification accuracy based on molecular data (>96%), a statistically significant
28 improvement (+2.1%) was observed. Detailed analysis of confusion rates between and
29 within genera shows that DNA alone tends to identify the genus correctly, but often fails
30 to recognize the species. The failure to resolve species is alleviated by including image data
31 in the training. This increase in resolution hints at a hierarchical role of modalities in
32 which molecular data coarsely groups the specimens to then be guided towards a more
33 fine-grained identification by the connected image. We systematically showed and
34 explained, for the first time, that optimizing the preprocessing and integration of molecular
35 and image data offers significant benefits, particularly for genetically similar and
36 morphologically indistinguishable species, enhancing species identification by reducing
37 modality-specific failure rates and information gaps. Our results can inform integration
38 efforts for various organism groups, improving automated identification across a wide range
39 of eukaryotic species.

40 *Key words:* data fusion, species identification, deep learning, DNA, images, integrative
41 taxonomy, species confusion

42

43 DNA has established itself as a widely used data source for automated species
44 identification efforts in both ecology and evolutionary research, helping to explore
45 evolutionary relationships and genetic diversity (Stuessy, 2009; Karbstein et al., 2024).
46 Traditionally, DNA-based species identification methods rely on short (approx. 1000 bp)
47 genetic markers known as barcodes that can be queried against large databases for species
48 identification (Hebert et al., 2003a; Ratnasingham and Hebert, 2007). Examples include
49 the NCBI nucleotide or the Barcode of Life initiative (BOLD) databases (Dietz et al.,
5 2023; Wiechers et al., 2023). Barcodes and the use of metabarcoding facilitate the
51 assessment of, e.g., environmental samples from aerobiological surveys to discern plant
52 species through pollen (Leontidou et al., 2021), or analyse biodiversity hotspots (Lahaye
53 et al., 2008; Bessey et al., 2020). Nevertheless, identification based on genetics can provide
54 suboptimal results in cases where sequences are too few or too short due to sampling or
55 sequencing issues, or where genetic regions are less variable due to strong pressures for
56 natural selection (Braukmann et al., 2017; Meiklejohn et al., 2019). Multi-locus analyses
57 have been repeatedly proposed to circumvent apparent drawbacks of single genetic
58 marker-based identification, ranging from two to hundreds of loci (Krawczyk et al., 2014;
59 Dietz et al., 2023). However, multi-locus compared to single-locus analyses increase lab
6 work and sequencing costs, are computationally more expensive, or are sometimes difficult
61 to interpret in case of gene tree conflicts (Karbstein et al., 2022; Dietz et al., 2023). In
62 recent years, machine learning (ML) and, in particular, deep learning (DL) approaches
63 have gained recognition in automatizing DNA-based tasks such as the identification or
64 delimitation of species (Zhang et al., 2008; Derkarabetian et al., 2019), DNA basecalling
65 (Boža et al., 2017), genome assembly polishing (Huang et al., 2021), and phylogenetic tree
66 building (Bhattacharjee and Bayzid, 2020).

67 Besides genetics, taxonomic research still largely relies on the study of
68 morphological characteristics. ML and, in particular, DL as a branch of ML have become

69 especially popular in the identification of species based on images (Buschbacher et al.,
7 2020; Mäder et al., 2021; van Klink et al., 2022; Green et al., 2023). This advancement can
71 be attributed to DL's ability to efficiently learn to recognize discriminatory, e.g., visual
72 patterns, which in turn enables the algorithm to evaluate the often extensive, feature-rich
73 biological datasets like diverse images of species (Wäldchen and Mäder, 2018).

74 Additionally, DL algorithms are becoming increasingly prevalent in image-based
75 species identification due to the availability of seminal network architectures such as
76 ResNet (He et al., 2016), which offer scientists a solid foundation for a myriad of derived
77 applications, especially in the automatic identification of different species groups
78 (Norouzzadeh et al., 2018; Mäder et al., 2021; Høye et al., 2021).

79 Image-based identification can either utilize *in situ*, i.e., field recorded (Terry et al.,
8 2020; Rzanny et al., 2022), specimens or preserved specimens from collections
81 (Carranza-Rojas et al., 2017; Marques et al., 2018; Hodač et al., 2023). The availability of
82 *in situ* images is rapidly increasing, particularly due to citizen science initiatives (Boho
83 et al., 2020; Mesaglio et al., 2023). Preserved specimens, represented by millions of samples
84 in natural history collections (Bebber et al., 2010; Scott and Livermore, 2021), have become
85 more relevant through increasing efforts to automate digitization (Blagoderov et al., 2012;
86 Tegelberg et al., 2014). Compared to genetics-based approaches, images from either *in situ*
87 or collection material provide a fast and low-cost means to species identification that can
88 reliably discriminate between species with a characteristic morphology (e.g. Mäder et al.,
89 2021; Shirai et al., 2022). Nevertheless, image-based species identification comes with its
9 own set of weaknesses, mainly introduced by cryptic species, high phenotypic plasticity,
91 and multiple origins of the same morphotype. These factors can also cause discrepancies
92 between systematics inferred from genetics and morphology, leading to revisions of former
93 morphospecies (e.g. Karbstein et al., 2020; Marcussen et al., 2022). Highly variable image
94 qualities and ways of recording further complicate identification and can lead to poor
95 identification accuracy, especially for species that are intrinsically hard to distinguish

96 (Wäldchen et al., 2018; Barbedo and Castro, 2019; Chiu et al., 2020).

97 To overcome the limitations of species identification using a single data point per
98 specimen, multiple data points either of the same modality or of different modalities can
99 be combined (e.g. Terry et al., 2020). Fusion of data can leverage machine learning
1 algorithms, which are adept at efficiently integrating disparate information (Karbstein
1.1 et al., 2024). Across disciplines, some attempts have been made to incorporate multiple
1.2 inputs into ML training. For example, the fusion of different image perspectives yields
1.3 enhanced results in terms of species identification accuracy (Marques et al., 2018; Rzanny
1.4 et al., 2022). On the other hand, integrative taxonomy seeks to overcome the limitations
1.5 outlined above by incorporating various types of data, thereby reducing modality-specific
1.6 (i.e., data type-specific) failure rates and information gaps (Dayrat, 2005; Schlick-Steiner
1.7 et al., 2010; Karbstein et al., 2024). While its utility has been limited by the large amount
1.8 of data required since traditional procedures rely on extensive pipelines that often include
1.9 manual labour and do not scale well, the application of machine learning methods offers a
11 solution. For instance, recent developments involve fusing with supplementary metadata
11.1 such as location or date (Terry et al., 2020). Nevertheless, particularly the integration of
11.2 DNA and image data emerges as a promising route to high-accuracy species identification.
11.3 So far, deep learning-assisted fusion of DNA and images has primarily been applied in
11.4 biomedical research (Stahlschmidt et al., 2022). To date, few studies have used genetic and
11.5 image input for species identification. Yang et al. (2022) have developed a new
11.6 convolution-based architecture for integrative species identification (MMNet) using
11.7 barcodes and images. They found that MMNet outperformed existing methods on 10
11.8 distinct datasets comprising both animal and plant groups while achieving very high
11.9 accuracies with up to 100% identification success. Badirli et al. (2023) used a hierarchical
12 Bayesian model to integrate DNA and image features of four insect orders derived from
12.1 unimodal convolutional neural networks (CNN). They found that multimodal species
12.2 identification performed better than unimodal ML methods but was surpassed by

123 traditional distance-based identification on DNA data. In addition, notable efforts in
124 species delimitation include the successful unsupervised training of a SuperSom, i.e., an
125 ANN producing a multi-layer grid, where each layer represents an input type
126 (Alexander Pyron, 2023). Another example is the use of a Bayesian approach that can
127 incorporate multiple loci and quantitative traits to suggest alternatives for provided
128 species labels (Solís-Lemus et al., 2015). Guillot et al. (2012) employ a statistical approach
129 with the goal of building homogeneous clusters without needing prior knowledge and using
130 spatial, phenotypic, and genetic information. Our exploration of the fundamental question
131 of how to preprocess genetic data for use with DL models and how to fuse genetic data
132 with other types of input extends the aforementioned studies.

133 Generally, DNA has to be specifically preprocessed in order to work with ML
134 methods. Multiple options of DNA arrangement and numerical encoding are imaginable.
135 Researchers can either choose to input sequences in their raw state, align them, or
136 additionally reduce them to single nucleotide polymorphisms (SNPs). DNA must also be
137 transformed into a numerical representation by turning each base into a vector of a chosen
138 length n , by assigning a specific numerical value to each base, or by learning an
139 informative representation. Such a representation can be learned using, for instance,
140 similarity learning approaches or, alternatively, a transformer architecture. Notable
141 examples of DNA-focused transformers are DNABERT (Ji et al., 2021) and DNAGPT
142 (Zhang et al., 2023). Transformers are powerful encoder-decoder structures that are
143 applied to text-like input. For comparability between the two modalities images and DNA,
144 we have opted to use CNNs instead. Additionally, there is a diverse range of deep learning
145 fusion methods (e.g. Seeland and Mäder, 2021). These methods encompass techniques such
146 as feature fusion, where features extracted from different modalities after any but the last
147 layer are combined to provide a more comprehensive representation of the data. Moreover,
148 score fusion aggregates predictions from multiple models or modalities to make a final
149 decision (Seeland and Mäder, 2021). To date, there has not been a systematic and

15 statistical comparison of DNA preprocessing and multimodal fusion approaches combining
151 genetic and image input applied across eukaryotes. Nonetheless, the choice for a
152 preprocessing and fusion method can enhance or limit both the achievable identification
153 accuracy and the efficiency of the model. For instance, reducing the DNA to SNPs can
154 decrease noise (e.g., missing data/gaps) and greatly accelerate training times when
155 working with very long sequences. Determining preprocessing and fusion methods that
156 yield consistently robust results across eukaryotic groups is, therefore, critical for species
157 identification efforts using ML. In addition, a comparison to the baseline, i.e., the accuracy
158 achieved by relying on a single datatype, is of importance as fusion always involves
159 additional effort and, thus, should only be considered when accompanied by a considerable
16 increase in identification accuracy. In this study, we use the genetic markers *COI* for two
161 animal and *rbcLa* for two plant families in combination with image-based morphological
162 data to systematically investigate preprocessing and fusion methods. In addition, we want
163 to provide future studies on integrative systematics with a baseline to guide them during
164 sample collection and the process of choosing an appropriate model architecture.
165 Specifically, we explore four key targets: 1) the determination of the DNA arrangement
166 and 2) encoding options that yield the most accurate species identification across diverse
167 datasets, 3) investigation of the impact that data fusion has on species identification
168 success, 4) assessment of the effectiveness of the proposed fusion strategies. Finally, we
169 explore the mechanisms underlying accuracy improvements resulting from the combination
17 of genetic and image data as a contribution to explainable AI.

171

MATERIAL AND METHODS

172

Dataset collection and filtering

173

174

175

We assembled four datasets, each comprising DNA and image data: two plant
datasets and two animal datasets (Table 1). Each dataset focuses on a specific family, with
varying numbers of genetic distances between and within genera and species to present

176 various levels of complexity with regard to differentiation. We gathered data from the
177 Asteraceae and the Poaceae family for the plant datasets. In the Poaceae dataset, we
178 utilized images captured in natural habitats, while for the Asteraceae dataset, we relied on
179 digitized herbarium material. This approach enabled us to examine the viability of our
180 method for *in situ* plant images as well as for digitized preserved specimens. The animal
181 datasets consist of the Coccinellidae and the Lycaenidae family. Due to data availability
182 constraints, we could only utilize images from preserved specimens, i.e., from collections,
183 for both datasets. For the same reason, we chose to set the minimum number of records
184 per species to four for all datasets, where each record is composed of a molecular and an
185 image sample. The low number of records reflects the reality many researchers face in their
186 sampling efforts (e.g., compare to Zarrei et al., 2015; Karbstein et al., 2020; Yang et al.,
187 2022). Although other papers such as (Badirli et al., 2023) have already collected datasets
188 comprising molecular and image data, we opted to gather our own. This decision was
189 motivated by our need for multiple datasets from both plants and animals, the intention to
190 include *in situ* and preserved material, and the nature of our research questions. Since we
191 were not interested in the total success rates of our models, but rather the relative gains
192 and losses between single- and multimodal trainings, we did not include any comparisons
193 to architectures proposed by other research papers. We have used the genetic markers
194 *COI-5P* for animals and *rbcLa* for plants. Although genome-level data would have been an
195 alternative to using genetic markers, they entail multiple challenges. First, DNA barcoding
196 has been a widely used method for species identification due to its relative efficiency in
197 terms of time, cost, and resources, which lead to extensive data collections and the
198 establishment of dedicated databases, such as BOLD (Ratnasingham and Hebert, 2007).
199 When selecting genetic markers, we considered both data availability and resource
200 efficiency, as well as how these choices would enhance the study's value for future research.
201 Second, additional formatting questions arise when working with genome-level data and
202 CNNs. Genome-level data is much more high-dimensional than the purposefully short

2 3 genetic markers and, thus, is more suited as input to alternative architectures and
 2 4 attention mechanisms (e.g., transformer) that can digest genome-level data more
 2 5 effectively. However, in this study, we actively decided on CNNs for their use in both
 2 6 image-based and DNA-based research. Implementing a CNN for both modalities facilitated
 2 7 an easy and valid comparison between models.

Table 1. Dataset overview. Datasets vary in the number of genera, species, and samples within the respective family. We relied on either *in situ* images or pictures from preserved specimens (collections). Information on the number of samples with related image and DNA data (combined) is listed alongside total sample size. We used *COI 5P* for both animal and *rbcLa* for the plant datasets. Mean gene lengths as well as standard deviations are listed as well. M=median. =mean

Family	No. of samples (combined)	Samples per species (M)	No. of species	Species per genus (M)	No. of genera	Barcode	Gene length ()	No. of SNPs	Image type
Asteraceae	970 (447)	5	146	1	45	<i>rbcLa</i>	550 (13)	106	collections
Poaceae	1118 (0)	7	123	1	54	<i>rbcLa</i>	555.9 (22)	114	<i>in situ</i>
Coccinellidae	1092 (683)	9	72	1	33	<i>COI 5P</i>	618.4 (59)	398	collections
Lycaenidae	5520 (2559)	8	259	1	98	<i>COI 5P</i>	645.3 (45)	482	collections

2 8 *Barcodes* We sourced all genetic data from publicly available repositories, namely
 2 9 BOLD (Barcode of Life Data Systems) and GenBank via their APIs. Our queries primarily
 21 relied on the family name. Since BOLD stores image and molecular data, we searched for
 211 combined records, i.e., 'specimen' and 'sequence'. GenBank does not offer image data.
 212 Thus, within our GenBank queries, we focused on 'genomic DNA/RNA' (property) and
 213 'gene or RNA' (feature key) data. Inspired by Paris et al. (2017) and Karbstein et al.
 214 (2020, 2021), we decided to assess and use sequence clustering and alignment features for
 215 filtering and to ensure a reasonable similarity between same-locus sequences. First, we
 216 ensured duplicate removal of GenBank records that were already sourced from BOLD by
 217 checking the GenBank accessions. Within each dataset, we then selected the five most
 218 abundant genetic markers. All associated sequences underwent clustering, with sequence
 219 similarity thresholds ranging from 0.5 (low similarity) to 0.99 (high similarity) in 0.01

22 increments using VSEARCH v2.22.1 (Rognes et al., 2016). To be able to keep as many
221 samples as possible, we conducted all further calculations on the largest cluster per
222 threshold. We determined the number of species and samples in this cluster as well as
223 generated an alignment with MAFFT v7.490 (Katoh and Standley, 2013) to compute the
224 SNP and gap counts relative to the aligned sequence length using SNP-sites v2.5.1 (Page
225 et al., 2016) and VCFtools v0.1.16 (Danecek et al., 2011). For each category (i.e., SNP and
226 gap), we then calculated the differences in values between the score of one threshold x and
227 the optimal score y . The optima represented the highest SNP and the lowest gap count
228 across all thresholds. To combine both aspects – SNP and gap counts – we calculated a
229 weighted mean, with double the emphasis on reducing the gap score. Finally, we chose the
23 threshold with the lowest combined divergence. Choosing a threshold based on a high SNP
231 and a low gap score allowed us to maximize the information content while ensuring that
232 our sequence clustering was correct.

233 Based on the chosen thresholds for each marker, we then decided on the genetic
234 marker for the respective dataset by considering the number of species retained in the
235 respective final datasets based on the chosen cluster and the average sample size per
236 species. Naturally, a high number of species leads to a more complex learning task while
237 the number of samples strongly impacts how well the model is able to distinguish between
238 classes, i.e. species (e.g. Durden et al., 2021). In detail, all values were sorted within their
239 respective property group, i.e., species number, and sample size. Based on these sorted
24 lists, we assigned numeric indices to each marker (e.g. first position in *species number* and
241 second in *sample size*). We picked the genetic marker with the lowest averaged index, i.e.,
242 the marker presenting the best possible balance between information content and inherent
243 task complexity introduced by many possible species. Our filtering resulted in the choice of
244 *COI-5P* for Coccinellidae and Lycaenidae, and *rbcLa* for Asteraceae and Poaceae with
245 identity thresholds set to 0.78, 0.88, 0.97, and 0.96 respectively. For clustering, we set the
246 maximum sequence length to 660 bp for *COI-5P* (Hebert et al., 2003b) and 670 bp for

247 *rbcLa* (Dong et al., 2014) respectively, while the minimum was set to 40% of the maximum
248 length. All sequences outside that range were discarded.

249 We observed duplicate sequences in all four datasets. As this is a known obstacle to
25 barcoding, especially in plants (Fazekas et al., 2009), we decided to regard duplicates as
251 naturally occurring identical sequences to more accurately represent the real world instead
252 of removing them from the dataset.

253 *Images* In addition to images obtained from BOLD, we collected further images
254 using the GBIF API. Similarly to the search for genetic and combined samples in BOLD,
255 our GBIF search was also based on the dataset family name. For the herbarium material
256 search in GBIF, we specified the basis of the record as 'preserved specimen' and 'material
257 sample'. In regards to *in situ* images, since most images deposited in BOLD depict
258 herbarium specimens, we decided to eliminate all BOLD-derived images before querying
259 other databases. We restricted GBIF results to iNaturalist research-grade observations as
26 well as including images from Flora Capture (Boho et al., 2020) to maximize the
261 trustworthiness of observations. Images from 'collections' belong to museums and
262 museum-acknowledged private collections that were labeled by experts instead of citizen
263 scientists as is the case for iNaturalist observations.

264 Duplicate images were automatically removed in both training and validation sets.
265 Regarding our validation sets, we ensured the following criteria in regards to image quality:
266 The image had to be of the correct type (i.e. showing *in situ* or preserved specimen) and
267 the sample needed to be the focus of the image. Images of low quality, i.e. visibly pixelated
268 images or images with no specimen depicted, were manually removed. Besides the removal
269 of duplicate images, we did not apply any filtering on the training sets. Our reasoning for
27 skipping further filtering steps on the training sets was as follows: A prominent goal when
271 leveraging online databases is to cut down on manual labor. Thus, being able to trust that
272 their derived large, heterogeneous datasets are of reasonable quality and can excel in the
273 context of ML is a vital aspect of future ventures into ML-assisted species identification.

274 *Experimental setup*

275 *Model architectures and BLAST* Both images and barcodes were trained using the
276 ResNet-50 architecture (He et al., 2016). ResNets, termed for their residual connections,
277 are seminal and widely adopted convolutional neural networks (CNNs) often chosen as a
278 baseline in computer vision projects (e.g. Mathur and Goel, 2021; De Nart et al., 2022).
279 CNNs are also prevalent in DNA-based research (e.g. Yang et al., 2022; Liu et al., 2022).
28 Here, we have used all 49 convolutional layers of the ResNet-50 as the feature extractor for
281 both unimodal model portions. Thus, our feature extractors have 23.5M parameters. For
282 the ordinal encoding, we prepended an embedding layer, composed of a 1x1 convolution
283 with a sliding window of 1 and no padding. The model’s input channel size was set to four
284 to accommodate the size of our fractional encoding vector and to one for the ordinal
285 encoding. The classifiers for our separate models have 1.8M parameters. For
286 comparability, we adjusted the number of parameters for the fused models to be twice the
287 size of the individual models. We have implemented all models using the framework
288 PyTorch v1.13.0+cu117 (Paszke et al., 2019) under Python v3.9.13. We trained on a Tesla
289 V100-SXM2 and a NVIDIA A40 GPU. Species identification was also performed using
29 *blastn* with default parameters (Camacho et al., 2009). To avoid bias from the extensive
291 records in the NCBI GenBank repository, locally created BLAST databases were used with
292 the BLAST+ *makeblastdb* command.

293 *Training* To prevent overfitting, we applied early stopping, i.e., stopping on the
294 training epoch that best generalized over the validation set, with a patience of 20 epochs
295 (Prechelt, 1998; Ying, 2019). The maximum number of epochs was set to 500. Following
296 Seeland and Mäder (2021) and derived from standard values, we applied categorical
297 cross-entropy loss with Adam as the optimizer, using an initial learning rate of 1e-4, and
298 set our mini-batch size to 32. Due to sample size constraints, we merely relied on the
299 validation set for performance evaluation. We validated model performances on two records

3 per species. All samples beyond that belong to the training sets. For images, we followed
3.1 standard procedures and applied common augmentation techniques (RandomResizedCrop,
3.2 RandomVerticalFlip, RandomHorizontalFlip). As a side effect of RandomResizedCrop,
3.3 most of the time, the model does not encounter the relatively small, but potentially
3.4 informative labels included in the images of preserved specimens. Since we were only
3.5 interested in determining which fusion approach performed best, label learning also did not
3.6 impact our conclusion. We optimized our Random Forest classifiers by applying grid search
3.7 to each of the datasets beforehand (Text S1). Our decision to optimize the Random Forest
3.8 was based on the much less time-consuming nature of the algorithm and the meager results
3.9 we attained in a preemptive test compared to the FC-based classifiers.

31 Our procedure included training on barcodes and images separately at first to
31.1 obtain a baseline for comparison. In image classification, it is a common procedure to
31.2 apply fine-tuning to pre-trained networks (e.g. Mathur et al., 2020; Kırbaş and Çifci,
31.3 2022). Here, our image model leveraged the ImageNet1K_V2-trained weights (Deng et al.,
31.4 2009). When training the multimodal model, we reused the weights acquired by the
31.5 unimodal training for both image and DNA data. We opted to freeze all layers but the last
31.6 block of the feature extractor during the second training step to concentrate on
31.7 higher-level feature learning (i.e., complex visual structures).

31.8 To test whether any differences in accuracy between the best fusion approaches and
31.9 the DNA- and image-only models were statistically significant, we implemented a
32 Leave-One-Out Cross-Validation (LOOCV) for all datasets (see Brownlee, 2020, for
32.1 detailed explanation). LOOCV is defined by running the model once for each sample in the
32.2 dataset. Every training uses the entire dataset except for one sample. Validation is then
32.3 performed on the excluded sample. However, due to time constraints, we decided to
32.4 validate on a subset of four samples per species for LOOCV. For example, we trained 4
32.5 (samples) times 146 (species) models for Asteraceae, summing up to 584 models per
32.6 uni-/multimodal method in total. Each model utilized all but one sample for training and

327 evaluated on the excluded sample. An alternative to using LOOCV would have been, e.g.,
328 a K-Fold Cross-Validation (K-Fold CV). With K-Fold CV, the dataset is split into K folds
329 or subsamples, where all but one fold are used for training and one fold is used to evaluate
33 the model's performance. Consequently, LOOCV is an extreme version of K-Fold CV.
331 While both approaches have their pros and cons, the very limited number of records per
332 species was the main reason we decided on LOOCV. Employing this approach, we also
333 conducted LOOCV for BLAST, creating the databases from all but one sample per dataset
334 and then querying the left-out sample against the database. Only the first listed hit was
335 considered for the accuracy calculation. To further test the stability of our limited
336 LOOCV, we conducted a more thorough LOOCV for one plant (Asteraceae) and one
337 animal (Coccinellidae) dataset that tested on all samples instead of the subset of 4. The
338 results are shown in Figures S1-S6.

339 *Metrics and statistics* We evaluated the performance of our models by means of
34 validation accuracy, i.e., the ratio of correctly classified samples to all samples in the
341 dataset. To check for significant differences in non-normally distributed accuracies within
342 all datasets, we employed the non-parametric, binary Cochran's Q test for datasets
343 characterized by more than two group factors and paired data using the R package
344 RVAideMemoire (Herve, 2023). Then, we performed pairwise group comparisons based on
345 the McNemar test to investigate differences in detail. Using R v4.3.1 (R Core Team, 2023)
346 and the caret package (Kuhn, 2008), we calculated confusion matrices based on our image,
347 barcode, and best multimodal model predictions to provide a basis for subsequent
348 analyses. We then determined confusion rates and grouped them by intergeneric and
349 intrageneric confusions. For the statistics on confusion rates, we applied the
35 non-parametric Kruskal-Wallis test for paired data in combination with pairwise Wilcoxon
351 signed rank tests. In addition, generalized linear models (GLMs) with binomial response
352 were used to check whether confusion rates are related to barcode (gene) length and
353 sample size using a custom R package. Using, in our case, confusion rates (species-level and

354 derived genus-level) as the response variable and different gene length features (min, max,
355 median) and sample size indices as the predictors, a custom package automates model
356 simplification. To avoid disturbance of modeling procedures (Dormann et al., 2013), the
357 main package function removes autocorrelated variables beforehand ($r > 0.8$; i.e., general
358 gene features and sample size indices to those indices in the training set). The
359 corresponding R scripts together with a README describing their explicit functions will
36 be available upon publication.

361 *Multimodal species identification scheme*

362 The workflow of our proposed multimodal species identification is illustrated in
363 Figure 1. It comprises three main steps: A) preprocessing of the DNA data, B) unimodal
364 species identification that serves as baseline and C) multimodal identification after
365 different fusion approaches of DNA and image data.

366 *DNA preprocessing* For automated species identification using DNA and deep
367 learning technologies, it is crucial to prepare the genetic data for input (arrangement) and
368 convert it into numerical representations (encoding). We refer to the combination of both
369 as DNA preprocessing. We examined three arrangements for genetic datasets: (i) aligning
37 DNA sequences, (ii) further reducing aligned sequences to SNPs, or (iii) padding the DNA
371 with zeros to the same length instead of aligning. As a result, we obtained three sequence
372 variants referred to as 'aligned', 'aligned-SNP', and 'unaligned' (Fig. 1 A(I)).

373 The arranged sequences are then encoded numerically before being subjected to
374 deep learning models (Fig. 1 A(II)). One approach is the fractional encoding, which is a
375 variant of the commonly used one-hot encoding method. For one-hot encoded
376 representation, the input sequence is represented by a $4 \times L$ matrix, where 4 is the size of
377 the bases vocabulary (A, T, C, and G) and L is the length of the sequence. Each position
378 in the sequence corresponds to a vector of length four, with a single non-zero element

379 representing the bases at that position. Specifically, the bases A, T, C, and G are encoded
380 as four one-hot vectors: $[1,0,0,0]$, $[0,1,0,0]$, $[0,0,1,0]$, and $[0,0,0,1]$. Therefore one-hot
381 encoding transforms DNA sequences into binary images with four channels corresponding
382 to A, C, G, and T. The special form of fractional encoding allows for values between 0 and
383 1. For instance, we encoded T as $[0,1,0,0]$, C as $[0,0,1,0]$, and Y (i.e., T or C) as
384 $[0,0.5,0.5,0]$. Gaps are encoded as zeros instead of extending the vector to maintain
385 consistency between aligned and unaligned sequences.

386 The second encoding method is an ordinal encoding, where decimal numbers
387 ranging from 0 to 1 are assigned to each of the bases. Instead of manually selecting them,
388 we let the model learn suitable decimals (see Model architectures for details). The optimal
389 combination of arrangement and encoding methods serves as the input for the subsequent
390 multimodal identification step.

391 *Unimodal baselines* To obtain a baseline with which to compare the results of the
392 multimodal approaches, genetic data and images were first trained individually. Here, we
393 extracted the features after the last CNN layer from the image- and DNA-trained models.
394 Subsequently, we passed the features through a classifier consisting of two fully connected
395 layers (see Fig. 1B). Additionally, the traditional method BLAST (Altschul et al., 1990)
396 was applied to assess whether it outperforms ML approaches for DNA-based species
397 identification.

398 *Multimodal fusion approaches* Multimodal fusion in our study refers to conducting
399 a combined analysis of molecular and image data to investigate whether the combination
400 yield a more accurate species identification result. Data fusion can be implemented at
401 different stages within the model architecture. Recently, it was demonstrated that
402 approaches fusing multiple image perspectives late in the network typically perform better
403 than those that fuse at an early stage (Seeland and Mäder, 2021). Similarly, in their review
404 on unimodal and multimodal fusion in the biomedical field, Stahlschmidt et al. (2022)

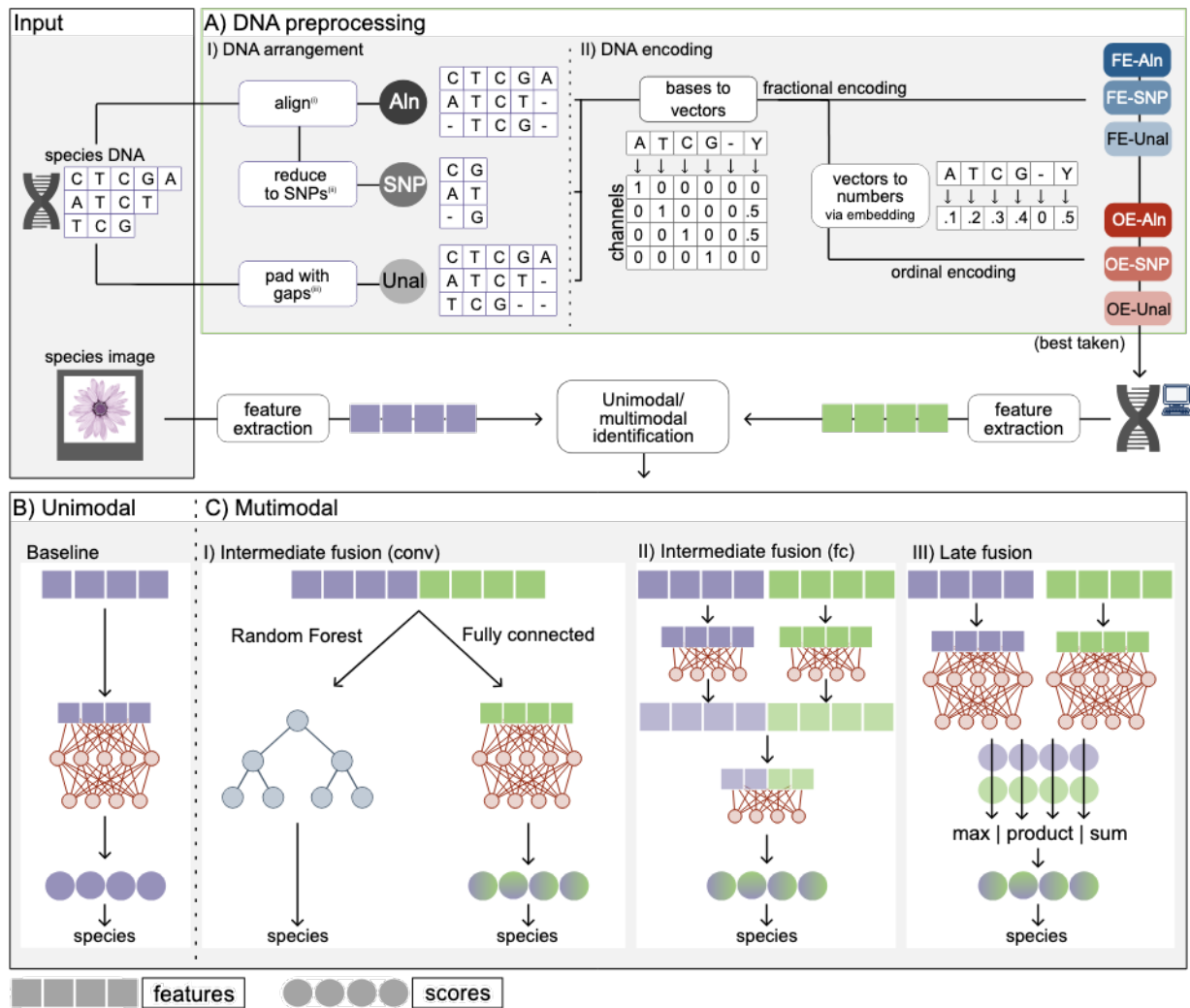


Fig. 1. Overview of the multimodal species identification scheme. A) DNA preprocessing route with different I) DNA arrangement and II) DNA encoding methods yielding six variations of the genetic model input in total. B) Unimodal identification with either image or DNA serve as baselines. C) Different fusion approaches for multimodal species identification I) image and DNA fusion after feature extraction (Intermediate fusion (conv)), II) after the first fully connected layer (Intermediate fusion (fc)), and III) after the second fully connected layer (late fusion). SNP = Single Nucleotide Polymorphisms, conv=convolution, fc=fully connected. (Preprocessed) DNA and flower images are from <https://pixabay.com> (free to use under the Content License).

4 5 noted that early fusion approaches often underperform when dealing with heterogeneous
 4 6 modalities. Consequently, we have combined the separate models within the last two layers
 4 7 of the network.

4 8 Specifically, we have fused image and barcode features I) directly after the last
 4 9 convolutional layer ('intermediate fusion (conv)'), II) after the first of two fully connected
 4 1 (i.e., dense) layers ('intermediate fusion (fc)') and III) after the final dense layer ('late')

411 responsible for generating the output scores (see Fig. 1C). Here, we expand on the
412 terminology used in Stahlschmidt et al. (2022). Instead of the two dense layers in the
413 intermediate fusion approach, we also employed a Random Forest (RF) using the
414 scikit-learn library to offer an easy and fast-to-train alternative to a fully connected
415 (fc)-based classifier (Pedregosa et al., 2011). Despite not being classified as neural
416 networks, they are highly capable of approximating any function and can learn non-linear
417 relationships (Hastie et al., 2009). In the score-level fusion approach, we examined three
418 methods: sum, product, and max score-level fusion. Therefore, we analyzed a total of six
419 different multimodal identification scenarios per dataset.

42 RESULTS

421 *DNA preprocessing methods*

422 Overall, DNA-based species identification was more accurate in the two animal
423 datasets (i.e., Coccinellidae, Lycaenidae) compared to the plant datasets (Asteraceae,
424 Poaceae; Fig. 2). Within the datasets, we observed significant differences in identification
425 accuracy between the arrangement and encoding methods. Notably, these differences
426 exhibit consistent patterns between all families. In both plant families, all arrangement
427 methods with ordinal encoding proved to be inferior compared to their respective
428 fractional encoding counterparts, with mean accuracies surpassing those of ordinal
429 encoding by 11% for Asteraceae and 13% for Poaceae. Within fractional encoding, padding
430 unaligned sequences resulted in the lowest identification rate (Asteraceae: 44.2%; Poaceae:
431 72%). In Poaceae, there was no significant difference between aligned and SNP-reduced
432 sequences, whereas in Asteraceae aligned sequences significantly outperformed
433 SNP-reduced sequences by 6%. The animal datasets yielded significantly higher
434 identification accuracy for aligned and SNP-reduced fractional encoded sequences than for
435 the remainder of the arrangement and encoding options (>6% improvement). The three
436 ordinal encoded and the unaligned fractional encoded barcodes provided similar results.

437 Similarly to Poaceae, there was no significant difference between aligned and aligned-SNP
438 sequences in Coccinellidae. In Lycaenidae, aligned sequences exceeded aligned-SNP
439 sequences in identification success (96.7% compared to 95%).

44 In both animal and plant datasets, fractional encoding performed better for aligned
441 and aligned-SNP sequences than ordinal encoding ($p < 0.0001$). For unaligned sequences,
442 fractional encoding was significantly better for the two plant groups ($p < 0.0001$) and the
443 Lycaenidae family ($p < 0.01$), whereas in the Coccinellidae family no significant differences
444 could be determined. For fractional encoding, unalignment resulted in a severe dip in
445 identification success compared to alignment ($p < 0.0001$). Furthermore, the magnitude of
446 the differences in accuracy between the preprocessing methods varied between datasets.
447 For example, in Poaceae and Coccinellidae, the biggest margin between two preprocessing
448 methods was between fractional encoded aligned sequences and ordinal encoded unaligned
449 sequences with 18% and 12%, respectively.

45 An expanded LOOCV that included all samples within the Asteraceae and
451 Coccinellidae datasets confirmed the results found when using the subsets. The only
452 difference observed was a minor change within the ordinal encoded sequences within the
453 Coccinellidae dataset, which shows that the unaligned sequences performed significantly
454 worse than the other two arrangements (Fig. S1).

455 *Unimodal species identification*

456 In a first step towards fusion and to obtain a baseline for the evaluation of our fusion
457 approaches, we trained on each modality separately. We observed significant differences
458 between models trained on images or DNA data across all datasets ($p < 0.0001$, Figure 3).
459 For the Poaceae dataset as well as the two animal datasets, the image-based model was
46 inferior to the one trained on DNA data. However, for the Asteraceae dataset, the
461 identification accuracy achieved by the model trained on images significantly exceeded the
462 DNA-only model, with 66.3% compared to 52.4%, respectively. For the Poaceae dataset,

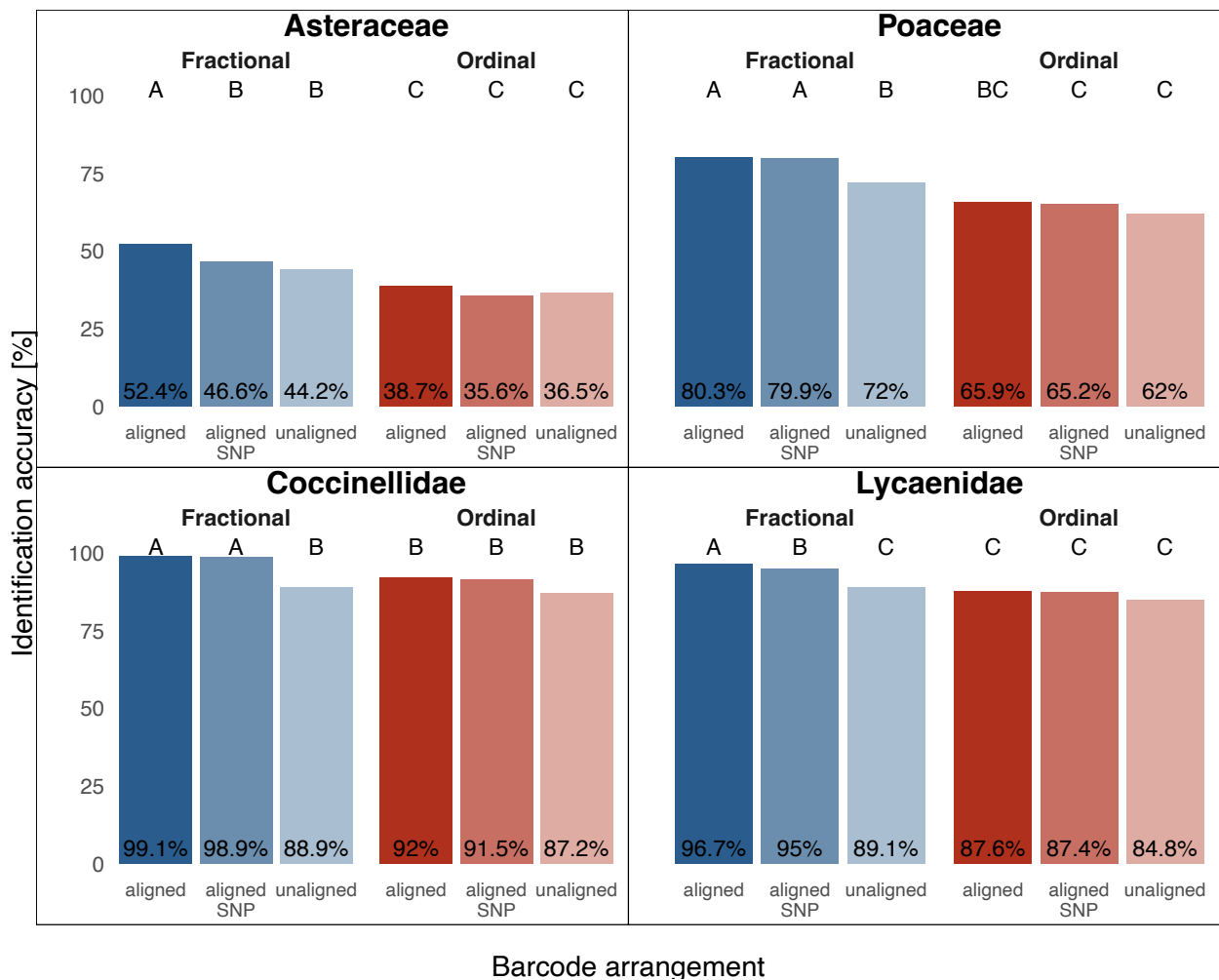


Fig. 2. DNA-based species identification accuracy after different arrangement (aligned, aligned-SNP, unaligned) and encoding (fractional, ordinal) methods for genetic data. Identification accuracy describes the percentage of samples within the validation set correctly identified by the model. Letters indicate significant differences in performance (paired Cochran's Q and pairwise McNemar's tests, $p < 0.001$). SNP = Single Nucleotide Polymorphisms.

463 DNA-based identification surpassed image-based identification by roughly 20% (80.3% and
 464 60.6%, respectively). Regarding the Coccinellidae, DNA-based identification achieved
 465 species identification with 99% accuracy, whereas images achieved sub-optimal results with
 466 81.3%. Similarly, in the Lycaenidae family, DNA data yielded 96.7% identification
 467 accuracy, while the image-based model identified 82.4% of samples correctly. In addition to
 468 our DL approach, we investigated the performance of BLAST, the traditional method for
 469 DNA-based species identification. BLAST's performance varied substantially across
 47 datasets. In the Asteraceae dataset, it misidentified more samples than the ML unimodal

471 image or DNA approaches, with only 33.4% correctly identified. In Poaceae, it performed
 472 similarly to the image-based model, achieving 58.3% identification accuracy. However, in
 473 Lycaenidae, BLAST outperformed images, achieving 91.7% accuracy, and in Coccinellidae,
 474 it achieved similar results to the DNA-based DL model, with a success rate of 98.6%.

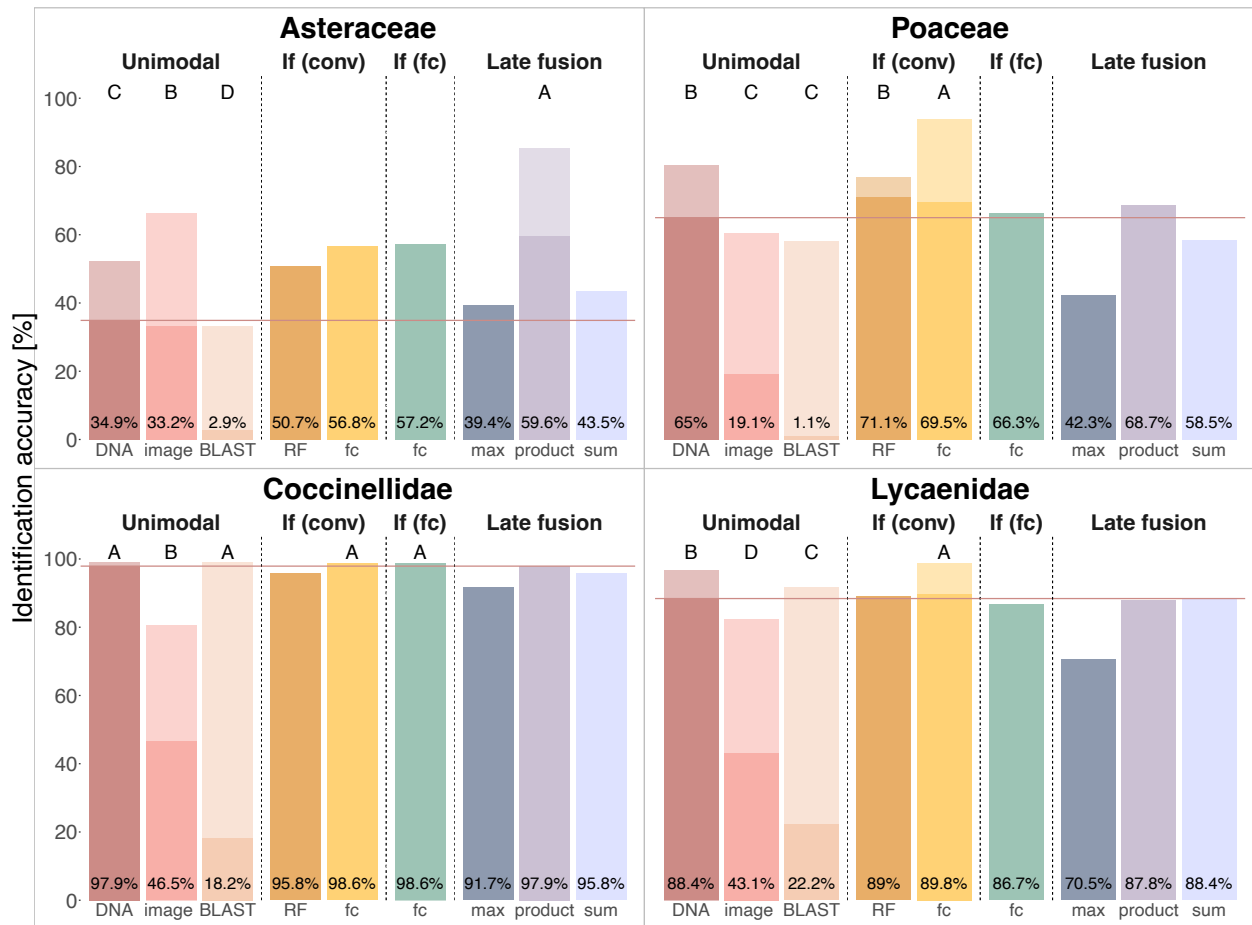


Fig. 3. Results of unimodal and multimodal species identification using different fusion approaches (If (conv), If (fc), Late fusion). Non-LOOCV training results and results of the traditional querying against a BLAST database are shown in saturated bars. The unimodal models, the traditional querying against a BLAST database, and the best fused model(s) were subjected to Leave-One-Out Cross-Validation (LOOCV; shown in light-colored bars). The distribution of identification success was statistically compared, resulting in letters indicating significant differences (paired Cochran's Q and pairwise McNemar's tests, $p < 0.001$), where A indicates the best performance and C/D the worst. The solid horizontal line illustrates the identification accuracy achieved by the superior unimodal model during the non-LOOCV training, reinforcing which of the multimodal models outperformed the unimodal models. If=Intermediate fusion, RF=Random Forest, fc=fully connected.

Multimodal species identification

Reusing the weights gained from training on a single modality (see Section Training), we combined the two modalities in a second training. In general, the fusion of DNA and image data outperformed unimodal species identification models across all datasets using the initial training and validation split (Fig. 3), with the increase in accuracy being more pronounced for the plant datasets than for the animal datasets. Product score fusion, as well as the intermediate (conv) and intermediate (fc) fusion approaches employing fully connected layers, consistently performed the best across datasets.

We validated our findings by applying LOOCV on both image- and DNA-only models as well as the fusion model(s) that yielded the highest success rate, i.e., product-score for Asteraceae, intermediate (conv) using a fully connected classifier for Poaceae, Coccinellidae, and Lycaenidae, and intermediate (fc) for Coccinellidae. In the Asteraceae dataset, both the DNA-based and image-based models exhibited a lower identification accuracy compared to the multimodal model. The score-level fusion approach using the score product outperformed the best unimodal model, the image-based model, by approximately 19% ($p < 0.0001$). Based on the initial training with the traditional training-validation split, we observed that the best fusion approach for all other datasets was the intermediate fusion (conv) approach using two fully connected layers for classification. In Poaceae, the intermediate fusion (conv) achieved a more accurate species identification compared to DNA alone ($p < 0.0001$) with 93.9% compared to 80.3%, respectively. Even when DNA-based models achieved very high identification success in the unimodal approach, as is the case for Lycaenidae (96.7%), we have been able to exceed the accuracy scores by using the intermediate fusion (conv) approach (98.8%, $p < 0.0001$). Only in Coccinellidae did both selected fusion methods not surpass the DNA-based model significantly. Here, the intermediate (conv) and intermediate (fc) fusion methods, the DNA-based model, and the approach using BLAST resulted in comparable identification

5 2 accuracies.

5 3 For both plant datasets, the baselines were still considerably lower than those of the
5 4 two animal groups. Thus, in plants, the fusion approaches that outperformed the unimodal
5 5 models do so by a large margin (Asteraceae: +19%; Poaceae: +13.6%). In animals, where
5 6 DNA-based models achieve very high accuracies on their own, the differences were less
5 7 pronounced (Lycaenidae: +2.1%).

5 8 The expanded LOOCV that included all samples within the Asteraceae and
5 9 Coccinellidae datasets confirmed the results of the subset-based approach (Fig. S2).

51 *Inter- and intrageneric confusion*

511 To understand which characteristics of the dataset may lead to low baseline
512 accuracies and to understand what effect the two modalities have on the model
513 performance, we compared intra- and intergeneric confusion rates. We observed middle to
514 low levels of misidentification per species across datasets and models with means ranging
515 from 0% to 37% per dataset (Table 2). In general, plants showed higher levels of
516 confusion compared to animals ($p < 0.0001$). DNA-based and fused models were
517 significantly less prone to confusing samples between genera than image-based models
518 (Asteraceae: $p < 0.0001$, Poaceae: $p < 0.0001$, Coccinellidae: $p < 0.05$, Lycaenidae: $p < 0.0001$).
519 In plants, barcodes and fused data were predominantly confused within rather than
520 between genera ($p < 0.0001$), while images tend to be confused more often between than
521 within genera ($p < 0.0001$). In animals, DNA is rarely confused with only 2.8% of species
522 showing any level of misidentification. Images, however, display the pattern observed in
523 plants and are more frequently misclassified on the level of genus than of species ($p < 0.05$).
524 Across datasets and confusion levels, the fusion approach that yielded the highest
525 identification accuracy delivers comparable results to the unimodal approach that performs
526 better (see Figure S7 for a per-genus perspective on confusion rates). The only exception
527 poses intrageneric confusion of Asteraceae images, where images alone are confused less

528 often than the combined modalities. However, in all other cases, fusion is a combination of
 529 the superior result of each modality. When investigating further and looking into duplicate
 530 sequences within all four datasets, DNA confusion was shown to be strongly linked to
 531 duplicates within and in between genera as revealed by Figure 4 (sample duplicate level:
 532 'intrageneric'/'intergeneric'). Particularly in Asteraceae and Poaceae, DNA samples were
 533 mainly falsely assigned to species that contained a duplicate to the respective sample in
 534 the training set (sample duplicate level: 'combi'). In all datasets, they were often confused
 535 with species that exclusively included duplicates and, therefore, had a genetic distance of
 536 0, or with species with very little genetic difference to the DNA sample. Oftentimes, these
 537 confusions could be solved by integrating image information since the genetic difference
 538 between true and assigned species was much larger when identifying using images.
 539 Information on samples that were only correctly identified by a single modality or not
 540 correctly identified at all is shown in Figures S8-S10.

Table 2. Results of paired Kruskal-Wallis and pairwise Wilcoxon signed rank tests for intergeneric (above) and intrageneric (below) confusion rates between tested modalities. Tests were applied to the confusion found during Leave-One-Out Cross-Validation (LOOCV). Letters indicate significant differences between modalities (A=highest confusion).

	Asteraceae	Poaceae	Coccinellidae	Lycaenidae
intergeneric confusion				
Kruskal	108.67	176.9	42.1	168
df	2	2	2	2
p-value	<0.0001	<0.0001	<0.0001	<0.0001
modality	mean confusion _{LOOCV}			
barcode	10.8% ^B	4.3 ^B	0.7 ^B	0.5 ^B
image	25%	36.8%	5.9%	11.9%
both	2.2 ^C	2.6 ^B	1.7 ^B	0.5 ^B
intrageneric confusion				
Kruskal	35.09	23.01	21.78	38.73
df	2	2	2	2
p-value	<0.0001	<0.0001	<0.0001	<0.0001
modality	mean confusion _{LOOCV}			
barcode	36.8%	15.4%	0.3 ^B	2.8% ^B
image	8.7 ^C	2.6 ^B	5.9%	5.7%
both	12.5% ^B	3.5 ^B	0 ^B	0.7 ^C

541 *Confusion in relation to gene length and sample size*

542 We found significant relationships between inter- and intrageneric confusion rates
543 and number of training samples and species within the genus as well as gene length (Table
544 S1). In detail, fewer samples were misidentified when the number of training samples was
545 larger in the following cases: a) Asteraceae, DNA-based model, intra- and intergeneric
546 ($p = 0.05$), b) Poaceae, image-based model, intrageneric ($p = 0.05$), and c) Lycaenidae,
547 image-based model, inter- and intrageneric ($p = 0.01$). The mean gene length and the
548 number of species within the genus had a significant impact on the confusion rate when
549 examining pooled data from all datasets. Here, the influence gene length has on confusion
55 was not conclusive in terms of positive/negative impact. For example, while a longer
551 validation gene length increases intrageneric confusion ($p = 0.001$), it decreases intergeneric
552 confusion in DNA-based species identification ($p = 0.0001$). In multimodal species
553 identification, the effect was positive for both intra- and intergeneric confusion ($p = 0.0001$
554 and $p = 0.05$, respectively). The number of species within the genus increases intrageneric
555 confusion levels of both DNA-based and multimodal models ($p = 0.001$, $p = 0.01$). Lastly, the
556 difference between the gene length in the training set compared to the validation set
557 impacted intrageneric confusion rates for DNA-based and multimodal models. However,
558 while the effect was positive in the DNA-based model ($p = 0.0001$), it was negative in
559 multimodal training ($p = 0.01$).

56 DISCUSSION

561 This study, for the first time, systematically analyzed various DNA preprocessing
562 methods and multimodal fusion approaches. We demonstrated that (i) fusion widely
563 outperforms unimodal identification, with fractional encoding of DNA combined with
564 intermediate (conv) and intermediate (fc) data fusion achieving the highest identification
565 accuracy in three out of four eukaryotic species groups, (ii) fusion significantly improved
566 identification even when genetic data yielded high species identification accuracy, (iii)

567 fusion reduces both high intrageneric confusion of barcode-based identification and high
568 intergeneric confusion of image-based identification.

569 *DNA preprocessing*

570 To date, there has not been an investigation on the effect of different DNA
571 preprocessing techniques. Yet, DNA preprocessing is a crucial step to ensure the efficiency
572 and effectiveness of a model. In this study, we compared six preprocessing methods. We
573 observed the most accurate species identification when first aligning the sequences before
574 applying fractional encoding in one plant and one animal dataset. This approach is
575 consistent with the practice of the majority of studies dealing with genetic data in the
576 context of ML while contrasting projects that rely on unaligned sequences for analyses
577 (e.g. Zhang et al., 2008; Fiannaca et al., 2018; Yang et al., 2022). Notably, we also found
578 that in Poaceae and Coccinellidae an additional step that reduces the aligned sequences to
579 their SNPs yielded results that were on par with the performance of complete sequences.
580 We conclude that the relative number of SNPs, i.e., the retained information, and its
581 balance with the loss of information that may arise by removing conservative regions is the
582 major factor contributing to the difference in performance between SNPs vs complete
583 alignments in some datasets. In detail, discarding conservative positions can disrupt
584 meaningful patterns that then form simpler patterns that, without the respective context,
585 are much more prevalent across locations within the sequence and between samples.
586 However, the success with using SNPs in Poaceae and Coccinellidae shows that SNPs can
587 be as informative as the complete sequence. This finding can contribute to model runtime
588 reduction efforts when dealing with large multi-gene datasets in future research. In
589 addition, the use of a non-CNN architecture that does not rely on recognizing patterns
590 within immediate local surroundings could improve the identification using SNPs. For
591 instance, transformers are a viable option for capturing non-local interactions as they use,
592 in contrast to ResNets, an attention mechanism (e.g. Ji et al., 2021).

Uni- and multimodal training

593

594 We have provided a fundamental comparison of fusion stages and classifiers that can
595 serve as a basis for future studies seeking a more holistic perspective on species identity
596 when training ML models. With respect to unimodal models, barcode-based models usually
597 yielded higher identification accuracy than image-based models. Notably, the identification
598 of plant species has proven to be much more challenging than the identification of animals,
599 with substantial differences in the ability to classify on barcodes alone. In Asteraceae, the
6 models based on barcodes were significantly outperformed by images. We attribute this to
6.1 the frequent occurrence of duplicate sequences in our plant datasets, particularly in the
6.2 Asteraceae dataset, which not only affects within-species confusion but also
6.3 misidentification between species or even genera. Events like apomixis, hybridization, and
6.4 polyploidy may contribute to this circumstance (Fazekas et al., 2009; Karbstein et al.,
6.5 2024). We discovered, however, that some of the cases in which species are confused due to
6.6 one or more duplicate sequences in the training set can be resolved by including the
6.7 information provided by the image. Our results show that the fusion of morphology and
6.8 genetics is usually beneficial, even when the genetic information itself is sufficient to
6.9 identify a vast majority of test samples. Fusing genetics with image data significantly
61 outperformed unimodal models for three out of four datasets. In Lycaenidae, fusion after
611 feature extraction with two shared fully connected layers outperformed the barcode-only
612 model by 2% while barcodes alone already classified 97% of samples correctly. While
613 identification accuracy did not increase with fusion in Coccinellidae, it is worth noting that
614 the dataset included fewer species and, at the median, more samples per species compared
615 to all other datasets, potentially rendering the task less difficult for the model. Overall,
616 integrating genetic and image features using a fully connected classifier consistently
617 produced the best or near-best results and therefore be recommended for integrative
618 species identification efforts. An explanation for the improvement brought by fusing
619 genetics with image data is the limited resolution of barcodes that has been discussed

several times in the past (Besse et al., 2021; Ahmed et al., 2022). The genes that we used
in this study were, on average, 550-650 bp long, while the median 1C-value (DNA in a
haploid nucleus) of, e.g., angiosperms, is 2.4 Gbp. Furthermore, plant genomes comprise
40,000 genes on average (Sterck et al., 2007). Considering this, a single gene is only a tiny
snapshot of the entire genome. In addition, natural selection acts on these DNA fragments,
reducing their variability and, in turn, their ability to differentiate closely-related species in
particular. In combination with the aforementioned intricate evolutionary processes, these
effects may result in large amounts of completely indistinguishable samples (Zarrei et al.,
2015; Karbstein et al., 2022). The stark contrast between accuracies achieved by animal
versus plant DNA-based models can be attributed to the specific markers used in this
study. When barcoding animals, *COI* represents the consensus due to its discriminatory
power (Hebert et al., 2003b; Ahmed et al., 2022). However, in plants, the mitochondrial
gene *COI* shows lower variation because it evolves too slowly in plants, therefore, nuclear
and plastid genes are used more often (Hollingsworth et al., 2011). Furthermore, it has
been shown that one marker alone tends to not be sufficient to distinguish between species
(Hollingsworth et al., 2016). Two or three markers are commonly used in conjunction to
provide fine-grained resolution (e.g. Romeiro-Brito et al., 2016). Consequently, a
substantially higher identification accuracy in animals compared to plants when using only
one plant marker is to be expected. Notably, the potential of an integrative approach to
species identification depends on the information already contained within each modality.
Researchers should choose carefully when opting for a multimodal, more time and resource
consuming approach by first assessing the relative gain of such a method, particularly
when working with animal DNA. Yet, the remaining, not sequenced DNA the network is
not trained on as well as environmental factors that reflect in epigenetics can be discernible
by the network through a condensed manifestation in the morphology of the specimen.
Our findings reinforce the direction proposed by Karbstein et al. (2024) for integrative
species delimitation and that there is a need for, at least, utilizing a multitude of genetic

647 and morphological information as well as metadata for accurate species delimitation (i.e.,
648 species delimitation 3.0). The identification accuracy achieved by using herbarium
649 material for the Asteraceae dataset proves that specimens from collections are a valuable
65 data source for integrative taxonomic ML approaches. Collection data has already started
651 to gain traction in biological ML research. For example, studies focusing on phenological
652 stage identification (Pearson et al., 2020; Katal et al., 2022), and plant organ segmentation
653 (Weaver and Smith, 2023) leverage herbarium material. Given that museum samples are
654 reliably labeled, even supervised learning algorithms can be applied without further work
655 necessary. Recently, features learned by an ML network and geometric
656 morphometrics-based features extracted manually from both *in situ* and herbarium
657 specimen images have been shown to be significantly correlated (Hodač et al., 2024),
658 demonstrating that ML is able to learn meaningful features from herbarium samples. Use
659 of collection material allows for cheaper studies with larger datasets and, potentially, more
66 robust results and should therefore be considered when working with ML. An important
661 aspect of this study is the usage of independent data points for DNA and images. Studies
662 such as Yang et al. (2022) use co-occurring data, i.e., DNA and image originate from the
663 same individual. Dependent data ensures that the variance experienced by the model is
664 part of the naturally occurring distribution, which may lead to better generalization when
665 confronted with other samples of the same distribution. Yet, this poses a vital problem as
666 co-occurring data can be hard to come by and, thus, can further limit and complicate
667 expensive dataset collection efforts. Consequently, no sampling effort will ever cover all
668 variance encountered within the naturally occurring distribution. When working with
669 images, a common procedure is data augmentation to semi-artificially increase the dataset
67 size and introduce more variation, which leads to better generalisation. Even when working
671 with DNA, data augmentation can improve model performance (Lee et al., 2023). When
672 working with multiple modalities, a way to augment the data can be to shuffle the
673 modalities independently, thereby creating more variation. Co-occurring data should

674 therefore not be a hard requirement for sampling e orts.

675 *Confusion*

676 Confusion patterns di er between images and barcodes. Images are oftentimes
677 confused between genera while barcodes tend to be confused within genera. In addition,
678 our findings suggest that datasets that contain species with significant genetic overlaps,
679 i.e., in cases where the barcoding gap is nearly or completely nonexistent, benefit the most
680 from inclusion of additional modalities. In those cases, these confusions could be solved by
681 integrating image information, highlighting the usefulness of an integrative taxonomic
682 approach to machine learning (Derkarabetian et al., 2019; Alexander Pyron, 2023;
683 Karbstein et al., 2024). Furthermore, cases in which either or both the molecular data and
684 the image alone did not suffice for a correct prediction but succeeded when used in tandem
685 hint towards a hierarchical role of the molecular data in the identification process. The
686 barcode may guide the model to the correct genus and then settle on the correct species
687 with the help of the image.

688 *Limitations*

689 The choice and quality of the genetic markers is an essential prerequisite to the
690 success of fusion approaches using ML. As seen, fusion was not able to outperform the
691 barcode-based approach in Coccinellidae as the baseline resolution provided by the
692 barcodes was close to perfect for the species in our dataset. The barcodes used in this study
693 were chosen based on the number of samples found in freely available online repositories.
694 We did not assess multiple barcodes for, e.g., the plant datasets, to confirm that no other
695 genetic marker would be better suited for species discrimination. However, *rbcLa* is widely
696 used in plant research, oftentimes in combination with *matK* (Li et al., 2015). In addition,
697 taxonomically challenging groups such as those where apomixis, hybridization, and/or
698 ploidy are prevalent pose a significant challenge to all plant barcodes (Fazekas et al., 2009;

699 Hollingsworth et al., 2016). We have shown that fusion can improve discrimination even in
7 groups where duplicate sequences are common. Therefore, irrespective of the marker used
7.1 in this study, we believe that these findings can be universally applied where species are
7.2 hard to distinguish by genetics alone. DL algorithms typically require substantial data to
7.3 perform effectively. While we acknowledge that the datasets our models were trained on
7.4 are relatively small, given the scarcity of many species groups, it becomes imperative to
7.5 explore and understand how ML models operate under conditions of limited data
7.6 availability. We are aware that the sample sizes of our datasets are not ideal for training
7.7 DL models, but believe that working with a limited amount of data is essential, as it
7.8 reflects the reality of taxonomy-focused studies (Karbstein et al., 2020; Klasen et al., 2022;
7.9 Opatova et al., 2024). Furthermore, our focus was not on the absolute accuracies attained
71 by our networks, but rather on the relative gains and losses between uni- and multimodal
711 models and different fusion strategies. Given that all models had access to the same
712 number of records, we consider the relative results to be unaffected by the total sample
713 size. Imbalanced sample sizes across classes, as is the case with all our datasets, cause some
714 features/classes to be trained more often than others, leading to model bias. However, as
715 all tested models were trained on the same data, model performance is comparable. We
716 also sampled our validation set evenly across classes to get a balanced look at identification
717 success. In addition, the learning process of ML models is still a 'black box' for human
718 observers. Although new explainable AI approaches are emerging to visualize and detect
719 biological features learned by the ML model (Samek et al., 2021; Hodač et al., 2024),
72 previous delimitation results from integrative taxonomy are needed, as well as experienced
721 taxonomists to control and validate ML-based species identification or clustering.

722

CONCLUSIONS

723

724

Modern integrative taxonomy aims to combine 21st century high-throughput sequencing (genomics) methods with multiple complementary data sources, such as

725 morphology from geometric morphometrics, ploidy reproduction from flow cytometry,
726 physiology from biochemical screenings, behavior from camera field observations, or
727 biogeography/ecology from environmental statistical modeling (Dayrat, 2005;
728 Schlick-Steiner et al., 2010; Karbstein et al., 2024). Modality-specific shortcomings are
729 reduced in this way, for example single, few, or even hundreds of genes are often not
730 variable enough to differentiate closely-related species (e.g. Tomasello et al., 2020; Dietz
731 et al., 2023) and therefore images of field or herbarium specimens, ploidy, reproductive,
732 behavioral, or ecological niche information can help to add subtle features for more
733 accurate and reliable species identification. As integrative taxonomy is a major avenue for
734 meeting the nature of species in (semi-)manual species delimitation (Dayrat, 2005;
735 Schlick-Steiner et al., 2010; Karbstein et al., 2020, 2022), the joint use of modalities should
736 also be considered a crucial pillar of any ML-based or -assisted approach to identification.
737 The rationale behind this lies in the fact that the taxonomic labels of the underlying
738 dataset are derived from the evaluation of multiple modalities. Consequently, future ML
739 studies should focus on evaluating >2 datasets to test generalizability across taxonomic
740 groups and >1 modality, preferably including >1 genetic marker to reflect delimitation
741 procedures.

742 This study paves the way by demonstrating, for the first time, that DNA+image
743 fusion strategies merging the features directly after the last convolution tend to yield the
744 best species identification success. Modern integrative taxonomic approaches produce
745 many, and often extraordinarily large datasets, which regularly cannot be handled by
746 traditional phylogenetic and statistical methods in time-efficient ways. DL approaches have
747 the advantage of automatically extracting and concentrating the most important, even
748 complex or subtle features not visible to the human eye for identification from extremely
749 large data matrices in short time frames (Borowiec et al., 2022; Badirli et al., 2023).
750 Consequently, future developments in data fusion are likely to accelerate integrative
751 taxonomic workflows for species identification and delimitation.

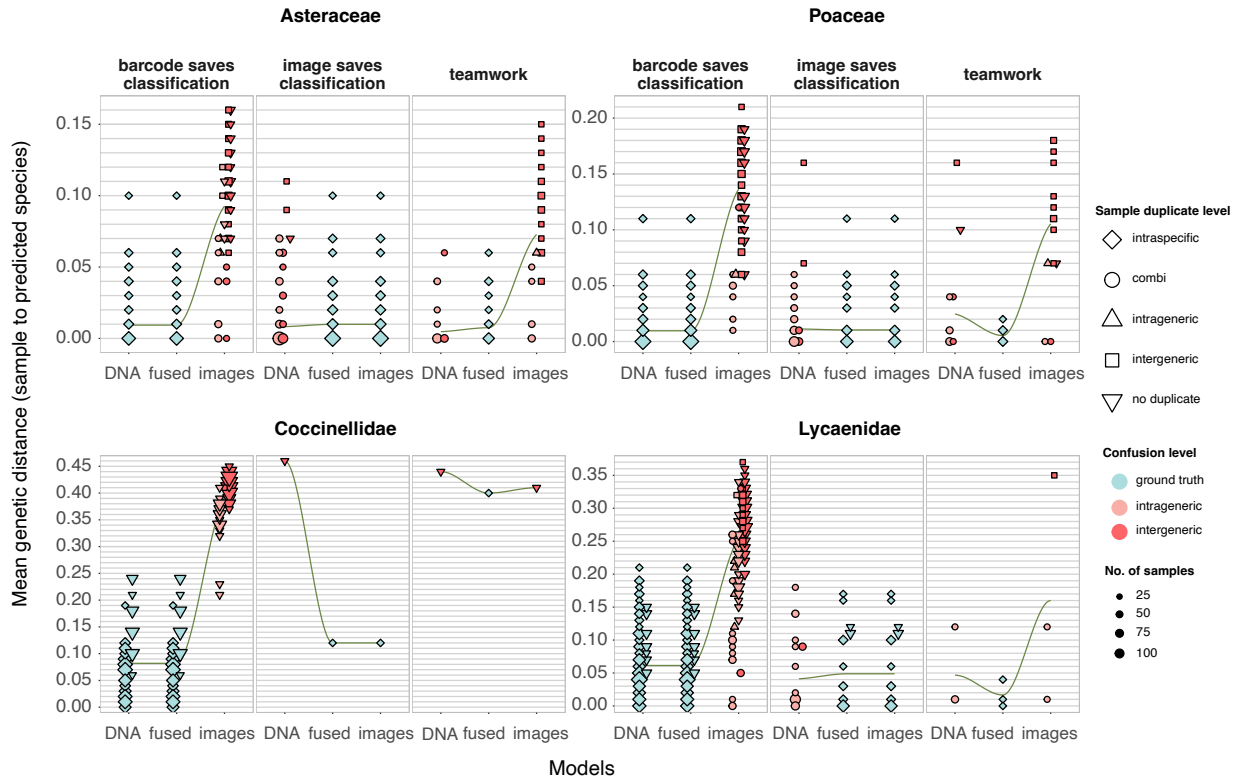


Fig. 4. Shown are confused samples that were either correctly identified by a) the barcode-only and (best) fused model, b) only the fused model, or c) the image-only and fused model. The y-axis displays the mean genetic distance (rounded to two decimal places) between the tested sample and the training samples of the predicted species. The level at which the samples were confused is indicated by the color; the shape provides information on whether and where there is a duplicate sequence in the training dataset. Numbers of samples matching genetic distance, duplicate status and confusion level are shown via data point size.

DATA AVAILABILITY

752

753 The authors declare that basic data supporting the findings will be available upon
754 publication.

755

FUNDING

756 This study was funded by the German Ministry of Education and Research
757 (BMBF) grant 01IS20062, the German Ministry of Agriculture and Food (BMEL-BLE)
758 grant 2819NA106, and the German Federal Ministry for the Environment, Nature
759 Conservation, Nuclear Safety, and Consumer Protection (BMUV) grant 67KI2086.

76

CONFLICT OF INTEREST

761 The authors declare no conflicts of interest.

762

REFERENCES

763 Ahmed, S., Ibrahim, M., Nantasenamat, C., Nisar, M.F., Malik, A.A., Waheed, R., Ahmed,
764 M.Z., Ojha, S.C., Alam, M.K., 2022. Pragmatic Applications and Universality of DNA
765 Barcoding for Substantial Organisms at Species Level: A Review to Explore a Way
766 Forward. *BioMed Research International* 2022, e1846485. doi:10.1155/2022/1846485.

767 Alexander Pyron, R., 2023. Unsupervised machine learning for species delimitation,
768 integrative taxonomy, and biodiversity conservation. *Molecular Phylogenetics and*
769 *Evolution* 189, 107939. doi:10.1016/j.ympcv.2023.107939.

77 Altschul, S.F., Gish, W., Miller, W., Myers, E.W., Lipman, D.J., 1990. Basic local
771 alignment search tool. *Journal of Molecular Biology* 215, 403–410.
772 doi:10.1016/S0022-2836(92)80360-2.

773 Badirli, S., Picard, C.J., Mohler, G., Richert, F., Akata, Z., Dundar, M., 2023. Classifying

- 774 the unknown: Insect identification with deep hierarchical Bayesian learning. *Methods in*
775 *Ecology and Evolution* 14, 1515–1530. doi:10.1111/2041-210X.14104.
- 776 Barbedo, J.G.A., Castro, G.B., 2019. Influence of image quality on the identification of
777 psyllids using convolutional neural networks. *Biosystems Engineering* 182, 151–158.
778 doi:10.1016/j.biosystemseng.2019.04.007.
- 779 Bebber, D.P., Carine, M.A., Wood, J.R.I., Wortley, A.H., Harris, D.J., Prance, G.T.,
780 Davidse, G., Paige, J., Pennington, T.D., Robson, N.K.B., Scotland, R.W., 2010.
781 Herbaria are a major frontier for species discovery. *Proceedings of the National*
782 *Academy of Sciences* 107, 22169–22171. doi:10.1073/pnas.1011841108.
- 783 Besse, P., Da Silva, D., Grisoni, M., 2021. Plant DNA Barcoding Principles and Limits: A
784 Case Study in the Genus *Vanilla*, in: Besse, P. (Ed.), *Molecular Plant Taxonomy: Methods and Protocols*. Springer US, New York, NY, pp. 131–148.
785 doi:10.1007/978-1-0716-0997-2_8.
- 787 Bessey, C., Jarman, S.N., Berry, O., Olsen, Y.S., Bunce, M., Simpson, T., Power, M.,
788 McLaughlin, J., Edgar, G.J., Keesing, J., 2020. Maximizing fish detection with eDNA
789 metabarcoding. *Environmental DNA* 2, 493–504. doi:10.1002/edn3.74.
- 790 Bhattacharjee, A., Bayzid, M.S., 2020. Machine learning based imputation techniques for
791 estimating phylogenetic trees from incomplete distance matrices. *BMC Genomics* 21,
792 1–14. doi:10.1186/s12864-020-06892-5.
- 793 Blagoderov, V., Kitching, I.J., Livermore, L., Simonsen, T.J., Smith, V.S., 2012. No
794 specimen left behind: Industrial scale digitization of natural history collections. *ZooKeys*
795 , 133–146doi:10.3897/zookeys.209.3178.
- 796 Boho, D., Rzanny, M., Wäldchen, J., Nitsche, F., Deggelmann, A., Wittich, H.C., Seeland,
797 M., Mäder, P., 2020. *Flora Capture*: A citizen science application for collecting

- 798 structured plant observations. *BMC Bioinformatics* 21, 1–11.
799 doi:10.1186/s12859-020-03920-9.
- 8 Borowiec, M.L., Dikow, R.B., Frandsen, P.B., McKeeken, A., Valentini, G., White, A.E.,
8 1 2022. Deep learning as a tool for ecology and evolution. *Methods in Ecology and*
8 2 *Evolution* 13, 1640–1660. doi:10.1111/2041-210X.13901.
- 8 3 Boža, V., Brejová, B., Vinař, T., 2017. DeepNano: Deep recurrent neural networks for base
8 4 calling in MinION nanopore reads. *PLOS ONE* 12, e0178751.
8 5 doi:10.1371/journal.pone.0178751.
- 8 6 Braukmann, T.W.A., Kuzmina, M.L., Sills, J., Zakharov, E.V., Hebert, P.D.N., 2017.
8 7 Testing the Efficacy of DNA Barcodes for Identifying the Vascular Plants of Canada.
8 8 *PLOS ONE* 12, e0169515. doi:10.1371/journal.pone.0169515.
- 8 9 Brownlee, J., 2020. LOOCV for Evaluating Machine Learning Algorithms. URL:
81 <https://machinelearningmastery.com/>
811 [loocv-for-evaluating-machine-learning-algorithms/](https://machinelearningmastery.com/loocv-for-evaluating-machine-learning-algorithms/).
- 812 Buschbacher, K., Ahrens, D., Espeland, M., Steinhage, V., 2020. Image-based species
813 identification of wild bees using convolutional neural networks. *Ecological Informatics*
814 55, 101017.
- 815 Camacho, C., Coulouris, G., Avagyan, V., Ma, N., Papadopoulos, J., Bealer, K., Madden,
816 T.L., 2009. BLAST+: Architecture and applications. *BMC bioinformatics* 10, 421.
817 doi:10.1186/1471-2105-10-421.
- 818 Carranza-Rojas, J., Goeau, H., Bonnet, P., Mata-Montero, E., Joly, A., 2017. Going
819 deeper in the automated identification of herbarium specimens. *BMC evolutionary*
82 *biology* 17, 1–14.
- 821 Chiu, T.Y., Zhao, Y., Gurari, D., 2020. Assessing Image Quality Issues for Real-World

- 822 Problems, in: 2020 IEEE/CVF Conference on Computer Vision and Pattern Recognition
823 (CVPR), pp. 3643–3653. doi:10.1109/CVPR42600.2020.00370.
- 824 Danecek, P., Auton, A., Abecasis, G., Albers, C.A., Banks, E., DePristo, M.A., Handsaker,
825 R.E., Lunter, G., Marth, G.T., Sherry, S.T., McVean, G., Durbin, R., 1000 Genomes
826 Project Analysis Group, 2011. The variant call format and VCFtools. *Bioinformatics* 27,
827 2156–2158. doi:10.1093/bioinformatics/btr330.
- 828 Dayrat, B., 2005. Towards integrative taxonomy. *Biological Journal of the Linnean Society*
829 85, 407–417. doi:10.1111/j.1095-8312.2005.00503.x.
- 83 De Nart, D., Costa, C., Di Prisco, G., Carpana, E., 2022. Image recognition using
831 convolutional neural networks for classification of honey bee subspecies. *Apidologie* 53,
832 5. doi:10.1007/s13592-022-00918-5.
- 833 Deng, J., Dong, W., Socher, R., Li, L.J., Li, K., Fei-Fei, L., 2009. ImageNet: A large-scale
834 hierarchical image database, in: 2009 IEEE Conference on Computer Vision and Pattern
835 Recognition, pp. 248–255. doi:10.1109/CVPR.2009.5206848.
- 836 Derkarabetian, S., Castillo, S., Koo, P.K., Ovchinnikov, S., Hedin, M., 2019. A
837 demonstration of unsupervised machine learning in species delimitation. *Molecular*
838 *Phylogenetics and Evolution* 139, 106562. doi:10.1016/j.ympev.2019.106562.
- 839 Dietz, L., Eberle, J., Mayer, C., Kukowka, S., Bohacz, C., Baur, H., Espeland, M., Huber,
84 B.A., Hutter, C., Mengual, X., Peters, R.S., Vences, M., Wesener, T., Willmott, K.,
841 Misof, B., Niehuis, O., Ahrens, D., 2023. Standardized nuclear markers improve and
842 homogenize species delimitation in Metazoa. *Methods in Ecology and Evolution* 14,
843 543–555. doi:10.1111/2041-210X.14041.
- 844 Dong, W., Cheng, T., Li, C., Xu, C., Long, P., Chen, C., Zhou, S., 2014. Discriminating
845 plants using the DNA barcode rbcLb: An appraisal based on a large data set. *Molecular*
846 *Ecology Resources* 14, 336–343. doi:10.1111/1755-0998.12185.

- 847 Dormann, C.F., Elith, J., Bacher, S., Buchmann, C., Carl, G., Carré, G., Marquéz, J.R.G.,
848 Gruber, B., Lafourcade, B., Leitão, P.J., Münkemüller, T., McClean, C., Osborne, P.E.,
849 Reineking, B., Schröder, B., Skidmore, A.K., Zurell, D., Lautenbach, S., 2013.
85 Collinearity: A review of methods to deal with it and a simulation study evaluating their
851 performance. *Ecography* 36, 27–46. doi:10.1111/j.1600-0587.2012.07348.x.
- 852 Durden, J.M., Hosking, B., Bett, B.J., Cline, D., Ruhl, H.A., 2021. Automated
853 classification of fauna in seabed photographs: The impact of training and validation
854 dataset size, with considerations for the class imbalance. *Progress in Oceanography* 196,
855 102612. doi:10.1016/j.pocean.2021.102612.
- 856 Fazekas, A.J., Kesanakurti, P.R., Burgess, K.S., Percy, D.M., Graham, S.W., Barrett,
857 S.C.H., Newmaster, S.G., Hajibabaei, M., Husband, B.C., 2009. Are plant species
858 inherently harder to discriminate than animal species using DNA barcoding markers?
859 *Molecular Ecology Resources* 9, 130–139. doi:10.1111/j.1755-0998.2009.02652.x.
- 86 Fiannaca, A., La Paglia, L., La Rosa, M., Lo Bosco, G., Renda, G., Rizzo, R., Gaglio, S.,
861 Urso, A., 2018. Deep learning models for bacteria taxonomic classification of
862 metagenomic data. *BMC Bioinformatics* 19, 198. doi:10.1186/s12859-018-2182-6.
- 863 Green, K.M., Virdee, M.K., Cubaynes, H.C., Aviles-Rivero, A.I., Fretwell, P.T., Gray,
864 P.C., Johnston, D.W., Schönlieb, C.B., Torres, L.G., Jackson, J.A., 2023. Gray whale
865 detection in satellite imagery using deep learning. *Remote Sensing in Ecology and*
866 *Conservation* 9, 829–840. doi:10.1002/rse2.352.
- 867 Guillot, G., Renaud, S., Ledevin, R., Michaux, J., Claude, J., 2012. A Unifying Model for
868 the Analysis of Phenotypic, Genetic, and Geographic Data. *Systematic Biology* 61,
869 897–911. doi:10.1093/sysbio/sys038.
- 87 Hastie, T., Tibshirani, R., Friedman, J., 2009. Random Forests, in: Hastie, T., Tibshirani,
871 R., Friedman, J. (Eds.), *The Elements of Statistical Learning: Data Mining, Inference,*

- 872 and Prediction. Springer, New York, NY, pp. 587–604.
873 doi:10.1007/978-0-387-84858-7_15.
- 874 He, K., Zhang, X., Ren, S., Sun, J., 2016. Deep Residual Learning for Image Recognition,
875 in: 2016 IEEE Conference on Computer Vision and Pattern Recognition (CVPR), IEEE,
876 Las Vegas, NV, USA. pp. 770–778. doi:10.1109/CVPR.2016.90.
- 877 Hebert, P.D., Ratnasingham, S., de Waard, J.R., 2003a. Barcoding animal life:
878 Cytochrome c oxidase subunit 1 divergences among closely related species. Proceedings
879 of the Royal Society of London. Series B: Biological Sciences 270, S96–S99.
88 doi:10.1098/rsbl.2003.0025.
- 881 Hebert, P.D.N., Cywinska, A., Ball, S.L., deWaard, J.R., 2003b. Biological identifications
882 through DNA barcodes. Proceedings of the Royal Society of London. Series B: Biological
883 Sciences 270, 313–321. doi:10.1098/rspb.2002.2218.
- 884 Herve, M., 2023. RVAideMemoire: Testing and Plotting Procedures for Biostatistics. URL:
885 <https://CRAN.R-project.org/package=RVAideMemoire>. r package version 0.9-83-7.
- 886 Hodač, L., Karbstein, K., Kösters, L., Rzanny, M., Wittich, H.C., Boho, D., Šubrt, D.,
887 Mäder, P., Wäldchen, J., 2024. Deep learning to capture leaf shape in plant images:
888 Validation by geometric morphometrics. The Plant Journal n/a.
889 doi:10.1111/tpj.17053.
- 89 Hodač, L., Karbstein, K., Tomasello, S., Wäldchen, J., Bradican, J.P., Hörandl, E., 2023.
891 Geometric Morphometric Versus Genomic Patterns in a Large Polyploid Plant Species
892 Complex. Biology 12, 418. doi:10.3390/biology12030418.
- 893 Hollingsworth, P.M., Graham, S.W., Little, D.P., 2011. Choosing and Using a Plant DNA
894 Barcode. PLOS ONE 6, e19254. doi:10.1371/journal.pone.0019254.
- 895 Hollingsworth, P.M., Li, D.Z., van der Bank, M., Twyford, A.D., 2016. Telling plant

- 896 species apart with DNA: From barcodes to genomes. *Philosophical Transactions of the*
897 *Royal Society B: Biological Sciences* 371, 20150338. doi:10.1098/rstb.2015.0338.
- 898 Høyve, T.T., Ärje, J., Bjerger, K., Hansen, O.L.P., Iosifidis, A., Leese, F., Mann, H.M.R.,
899 Meissner, K., Melvad, C., Raitoharju, J., 2021. Deep learning and computer vision will
9 transform entomology. *Proceedings of the National Academy of Sciences* 118,
9.1 e2002545117. doi:10.1073/pnas.2002545117.
- 9.2 Huang, N., Nie, F., Ni, P., Luo, F., Gao, X., Wang, J., 2021. NeuralPolish: A novel
9.3 Nanopore polishing method based on alignment matrix construction and orthogonal
9.4 Bi-GRU Networks. *Bioinformatics* 37, 3120–3127.
9.5 doi:10.1093/bioinformatics/btab354.
- 9.6 Ji, Y., Zhou, Z., Liu, H., Davuluri, R.V., 2021. DNABERT: Pre-trained Bidirectional
9.7 Encoder Representations from Transformers model for DNA-language in genome.
9.8 *Bioinformatics* 37, 2112–2120. doi:10.1093/bioinformatics/btab083.
- 9.9 Karbstein, K., Kösters, L., Hodač, L., Hofmann, M., Hörandl, E., Tomasello, S., Wagner,
91 N.D., Emerson, B.C., Albach, D.C., Scheu, S., Bradler, S., de Vries, J., Irisarri, I., Li, H.,
911 Soltis, P., Mäder, P., Wäldchen, J., 2024. Species delimitation 4.0: Integrative taxonomy
912 meets artificial intelligence. *Trends in Ecology & Evolution* 39, 771–784.
913 doi:10.1016/j.tree.2023.11.002.
- 914 Karbstein, K., Tomasello, S., Hodač, L., Dunkel, F.G., Daubert, M., Hörandl, E., 2020.
915 Phylogenomics supported by geometric morphometrics reveals delimitation of sexual
916 species within the polyploid apomictic *Ranunculus auricomus* complex (Ranunculaceae).
917 *TAXON* 69, 1191–1220. doi:10.1002/tax.12365.
- 918 Karbstein, K., Tomasello, S., Hodač, L., Lorberg, E., Daubert, M., Hörandl, E., 2021.
919 Moving beyond assumptions: Polyploidy and environmental effects explain a
92 geographical parthenogenesis scenario in European plants. *Molecular Ecology* 30,
921 2659–2675. doi:10.1111/mec.15919.

- 922 Karbstein, K., Tomasello, S., Hodač, L., Wagner, N., Marinček, P., Barke, B.H., Paetzold,
923 C., Hörandl, E., 2022. Untying Gordian knots: Unraveling reticulate polyploid plant
924 evolution by genomic data using the large *Ranunculus auricomus* species complex. *New*
925 *Phytologist* 235, 2081–2098. doi:10.1111/nph.18284.
- 926 Katal, N., Rzanny, M., Mäder, P., Wäldchen, J., 2022. Deep Learning in Plant
927 Phenological Research: A Systematic Literature Review. *Frontiers in Plant Science* 13.
928 doi:10.3389/fpls.2022.805738.
- 929 Katoh, K., Standley, D.M., 2013. MAFFT Multiple Sequence Alignment Software Version
93 7: Improvements in Performance and Usability. *Molecular Biology and Evolution* 30,
931 772–780. doi:10.1093/molbev/mst010.
- 932 Kirbaş, İ., Çifci, A., 2022. An effective and fast solution for classification of wood species:
933 A deep transfer learning approach. *Ecological Informatics* 69, 101633.
934 doi:10.1016/j.ecoinf.2022.101633.
- 935 Klasen, M., Ahrens, D., Eberle, J., Steinhage, V., 2022. Image-Based Automated Species
936 Identification: Can Virtual Data Augmentation Overcome Problems of Insufficient
937 Sampling? *Systematic Biology* 71, 320–333. doi:10.1093/sysbio/syab048.
- 938 van Klink, R., August, T., Bas, Y., Bodesheim, P., Bonn, A., Fossøy, F., Høye, T.T.,
939 Jongejans, E., Menz, M.H.M., Miraldo, A., Roslin, T., Roy, H.E., Ruczyński, I., Schigel,
94 D., Schäffler, L., Sheard, J.K., Svenningsen, C., Tschan, G.F., Wäldchen, J., Zizka,
941 V.M.A., Åström, J., Bowler, D.E., 2022. Emerging technologies revolutionise insect
942 ecology and monitoring. *Trends in Ecology & Evolution* 37, 872–885.
943 doi:10.1016/j.tree.2022.06.001.
- 944 Krawczyk, K., Szczecińska, M., Sawicki, J., 2014. Evaluation of 11 single-locus and seven
945 multilocus DNA barcodes in *Lamium* L. (Lamiaceae). *Molecular Ecology Resources* 14,
946 272–285. doi:10.1111/1755-0998.12175.

- 947 Kuhn, M., 2008. Building Predictive Models in R Using the caret Package. *Journal of*
948 *Statistical Software* 28, 1–26. doi:10.18637/jss.v028.i05.
- 949 Lahaye, R., van der Bank, M., Bogarin, D., Warner, J., Pupulin, F., Gigot, G., Maurin, O.,
95 Duthoit, S., Barraclough, T.G., Savolainen, V., 2008. DNA barcoding the floras of
951 biodiversity hotspots. *Proceedings of the National Academy of Sciences* 105, 2923–2928.
952 doi:10.1073/pnas.0709936105.
- 953 Lee, N.K., Tang, Z., Toneyan, S., Koo, P.K., 2023. EvoAug: Improving generalization and
954 interpretability of genomic deep neural networks with evolution-inspired data
955 augmentations. *Genome Biology* 24, 1–14. doi:10.1186/s13059-023-02941-w.
- 956 Leontidou, K., Vokou, D., Sandionigi, A., Bruno, A., Lazarina, M., De Groeve, J., Li, M.,
957 Varotto, C., Girardi, M., Casiraghi, M., Cristofori, A., 2021. Plant biodiversity
958 assessment through pollen DNA metabarcoding in Natura 2000 habitats (Italian Alps).
959 *Scientific Reports* 11, 18226. doi:10.1038/s41598-021-97619-3.
- 96 Li, X., Yang, Y., Henry, R.J., Rossetto, M., Wang, Y., Chen, S., 2015. Plant DNA
961 barcoding: From gene to genome. *Biological Reviews* 90, 157–166.
962 doi:10.1111/brv.12104.
- 963 Liu, X., Xu, Y., Luo, Y., Teng, L., 2022. Prokaryotic and eukaryotic promoters
964 identification based on residual network transfer learning. *Bioprocess and Biosystems*
965 *Engineering* 45, 955–967. doi:10.1007/s00449-022-02716-w.
- 966 Mäder, P., Boho, D., Rzanny, M., Seeland, M., Wittich, H.C., Deggelmann, A., Wäldchen,
967 J., 2021. The Flora Incognita app – Interactive plant species identification. *Methods in*
968 *Ecology and Evolution* 12, 1335–1342. doi:10.1111/2041-210X.13611.
- 969 Marcussen, T., Ballard, H.E., Danihelka, J., Flores, A.R., Nicola, M.V., Watson, J.M.,
97 2022. A Revised Phylogenetic Classification for Viola (Violaceae). *Plants* 11, 2224.
971 doi:10.3390/plants11172224.

- 972 Marques, A.C.R., Raimundo, M.M., Cavalheiro, E.M.B., Salles, L.F.P., Lyra, C., Zuben,
973 F.J.V., 2018. Ant genera identification using an ensemble of convolutional neural
974 networks. *PLOS ONE* 13, e0192011. doi:10.1371/journal.pone.0192011.
- 975 Mathur, M., Goel, N., 2021. FishResNet: Automatic Fish Classification Approach in
976 Underwater Scenario. *SN Computer Science* 2, 273. doi:10.1007/s42979-021-00614-8.
- 977 Mathur, M., Vasudev, D., Sahoo, S., Jain, D., Goel, N., 2020. Crosspooled FishNet:
978 Transfer learning based fish species classification model. *Multimedia Tools and*
979 *Applications* 79, 31625–31643. doi:10.1007/s11042-020-09371-x.
- 98 Meiklejohn, K.A., Damaso, N., Robertson, J.M., 2019. Assessment of BOLD and GenBank
981 – Their accuracy and reliability for the identification of biological materials. *PLOS ONE*
982 14, e0217084. doi:10.1371/journal.pone.0217084.
- 983 Mesaglio, T., Sauquet, H., Coleman, D., Wenk, E., Cornwell, W.K., 2023. Photographs as
984 an essential biodiversity resource: drivers of gaps in the vascular plant photographic
985 record. *New Phytologist* 238, 1685–1694.
- 986 Norouzzadeh, M.S., Nguyen, A., Kosmala, M., Swanson, A., Palmer, M.S., Packer, C.,
987 Clune, J., 2018. Automatically identifying, counting, and describing wild animals in
988 camera-trap images with deep learning. *Proceedings of the National Academy of*
989 *Sciences* 115, E5716–E5725. doi:10.1073/pnas.1719367115.
- 99 Opatova, V., Bourguignon, K., Bond, J.E., 2024. Species delimitation with limited
991 sampling: An example from rare trapdoor spider genus *Cyclocosmia* (Mygalomorphae,
992 Halonoproctidae). *Molecular Ecology Resources* 24, e13894.
993 doi:10.1111/1755-0998.13894.
- 994 Page, A.J., Taylor, B., Delaney, A.J., Soares, J., Seemann, T., Keane, J.A., Harris, S.R.,
995 2016. SNP-sites: Rapid efficient extraction of SNPs from multi-FASTA alignments.
996 *Microbial Genomics* 2, e000056. doi:10.1099/mgen.0.000056.

- 997 Paris, J.R., Stevens, J.R., Catchen, J.M., 2017. Lost in parameter space: A road map for
998 stacks. *Methods in Ecology and Evolution* 8, 1360–1373.
999 doi:10.1111/2041-210X.12775.
- 1 Paszke, A., Gross, S., Massa, F., Lerer, A., Bradbury, J., Chanan, G., Killeen, T., Lin, Z.,
1 1 Gimelshein, N., Antiga, L., Desmaison, A., Köpf, A., Yang, E., DeVito, Z., Raison, M.,
1 2 Tejani, A., Chilamkurthy, S., Steiner, B., Fang, L., Bai, J., Chintala, S., 2019. PyTorch:
1 3 An imperative style, high-performance deep learning library, in: *Proceedings of the 33rd*
1 4 *International Conference on Neural Information Processing Systems*. Curran Associates
1 5 Inc., Red Hook, NY, USA. 721, pp. 8026–8037.
- 1 6 Pearson, K.D., Nelson, G., Aronson, M.F.J., Bonnet, P., Brenskelle, L., Davis, C.C.,
1 7 Denny, E.G., Ellwood, E.R., Goëau, H., Heberling, J.M., Joly, A., Lorieul, T., Mazer,
1 8 S.J., Meineke, E.K., Stucky, B.J., Sweeney, P., White, A.E., Soltis, P.S., 2020. Machine
1 9 Learning Using Digitized Herbarium Specimens to Advance Phenological Research.
1 1 *BioScience* 70, 610–620. doi:10.1093/biosci/biaa044.
- 1 11 Pedregosa, F., Varoquaux, G., Gramfort, A., Michel, V., Thirion, B., Grisel, O., Blondel,
1 12 M., Prettenhofer, P., Weiss, R., Dubourg, V., Vanderplas, J., Passos, A., Cournapeau,
1 13 D., Brucher, M., Perrot, M., Duchesnay, É., 2011. Scikit-learn: Machine Learning in
1 14 Python. *Journal of Machine Learning Research* 12, 2825–2830.
- 1 15 Prechelt, L., 1998. Automatic early stopping using cross validation: Quantifying the
1 16 criteria. *Neural Networks* 11, 761–767. doi:10.1016/S0893-6080(98)00010-0.
- 1 17 R Core Team, 2023. R: A Language and Environment for Statistical Computing. R
1 18 Foundation for Statistical Computing. Vienna, Austria. URL:
1 19 <https://www.R-project.org/>.
- 1 20 Ratnasingham, S., Hebert, P.D.N., 2007. Bold: The Barcode of Life Data System
1 21 (<http://www.barcodinglife.org>). *Molecular Ecology Notes* 7, 355–364.
1 22 doi:10.1111/j.1471-8286.2007.01678.x.

- 1 23 Rognes, T., Flouri, T., Nichols, B., Quince, C., Mahé, F., 2016. VSEARCH: A versatile
1 24 open source tool for metagenomics. *PeerJ* 4, e2584. doi:10.7717/peerj.2584.
- 1 25 Romeiro-Brito, M., Moraes, E.M., Taylor, N.P., Zappi, D.C., Franco, F.F., 2016.
1 26 Lineage-specific evolutionary rate in plants: Contributions of a screening for *Cereus*
1 27 (*Cactaceae*). *Applications in Plant Sciences* 4, 1500074. doi:10.3732/apps.1500074.
- 1 28 Rzanny, M., Wittich, H.C., Mäder, P., Deggelmann, A., Boho, D., Wäldchen, J., 2022.
1 29 Image-Based Automated Recognition of 31 Poaceae Species: The Most Relevant
1 3 Perspectives. *Frontiers in Plant Science* 12.
- 1 31 Samek, W., Montavon, G., Lapuschkin, S., Anders, C.J., Müller, K.R., 2021. Explaining
1 32 Deep Neural Networks and Beyond: A Review of Methods and Applications.
1 33 *Proceedings of the IEEE* 109, 247–278. doi:10.1109/JPROC.2021.3060483.
- 1 34 Schlick-Steiner, B.C., Steiner, F.M., Seifert, B., Stauer, C., Christian, E., Crozier, R.H.,
1 35 2010. Integrative Taxonomy: A Multisource Approach to Exploring Biodiversity. *Annual*
1 36 *Review of Entomology* 55, 421–438. doi:10.1146/annurev-ento-112408-085432.
- 1 37 Scott, B., Livermore, L., 2021. Extracting Data at Scale: Machine learning at the Natural
1 38 History Museum. *Biodiversity Information Science and Standards* 5, e74031.
1 39 doi:10.3897/biss.5.74031.
- 1 4 Seeland, M., Mäder, P., 2021. Multi-view classification with convolutional neural networks.
1 41 *PLOS ONE* 16, e0245230. doi:10.1371/journal.pone.0245230.
- 1 42 Shirai, M., Takano, A., Kurosawa, T., Inoue, M., Tagane, S., Tanimoto, T., Koganeyama,
1 43 T., Sato, H., Terasawa, T., Horie, T., Mandai, I., Akihiro, T., 2022. Development of a
1 44 system for the automated identification of herbarium specimens with high accuracy.
1 45 *Scientific Reports* 12, 8066. doi:10.1038/s41598-022-11450-y.
- 1 46 Solís-Lemus, C., Knowles, L.L., Ané, C., 2015. Bayesian species delimitation combining

- 1 47 multiple genes and traits in a unified framework. *Evolution* 69, 492–507.
1 48 doi:10.1111/evo.12582.
- 1 49 Stahlschmidt, S.R., Ulfenborg, B., Synnergren, J., 2022. Multimodal deep learning for
1 5 biomedical data fusion: A review. *Briefings in Bioinformatics* 23, bbab569.
1 51 doi:10.1093/bib/bbab569.
- 1 52 Sterck, L., Rombauts, S., Vandepoele, K., Rouzé, P., Van de Peer, Y., 2007. How many
1 53 genes are there in plants (... and why are they there)? *Current Opinion in Plant*
1 54 *Biology* 10, 199–203. doi:10.1016/j.pbi.2007.01.004.
- 1 55 Stuessy, T.F., 2009. *Plant Taxonomy: The Systematic Evaluation of Comparative Data*.
1 56 Columbia University Press.
- 1 57 Tegelberg, R., Mononen, T., Saarenmaa, H., 2014. High-performance digitization of
1 58 natural history collections: Automated imaging lines for herbarium and insect
1 59 specimens. *TAXON* 63, 1307–1313. doi:10.12705/636.13.
- 1 6 Terry, J.C.D., Roy, H.E., August, T.A., 2020. Thinking like a naturalist: Enhancing
1 61 computer vision of citizen science images by harnessing contextual data. *Methods in*
1 62 *Ecology and Evolution* 11, 303–315. doi:10.1111/2041-210X.13335.
- 1 63 Tomasello, S., Karbstein, K., Hodač, L., Paetzold, C., Hörandl, E., 2020. Phylogenomics
1 64 unravels Quaternary vicariance and allopatric speciation patterns in temperate-montane
1 65 plant species: A case study on the *Ranunculus auricomus* species complex. *Molecular*
1 66 *Ecology* 29, 2031–2049. doi:10.1111/mec.15458.
- 1 67 Wäldchen, J., Mäder, P., 2018. Machine learning for image based species identification.
1 68 *Methods in Ecology and Evolution* 9, 2216–2225. doi:10.1111/2041-210X.13075.
- 1 69 Wäldchen, J., Rzanny, M., Seeland, M., Mäder, P., 2018. Automated plant species
1 7 identification—trends and future directions. *PLoS computational biology* 14, e1005993.

- 1 71 Weaver, W.N., Smith, S.A., 2023. From leaves to labels: Building modular machine
1 72 learning networks for rapid herbarium specimen analysis with LeafMachine2.
1 73 Applications in Plant Sciences 11, e11548. doi:10.1002/aps3.11548.
- 1 74 Wiechers, S., Kösters, L.M., Quandt, D., Borsch, T., Wicke, S., Müller, K.F., 2023.
1 75 BarKeeper—a versatile web framework to assemble, analyse and manage DNA
1 76 barcoding data and metadata. Methods in Ecology and Evolution 14, 799–805.
1 77 doi:10.1111/2041-210X.14047.
- 1 78 Yang, B., Zhang, Z., Yang, C.Q., Wang, Y., Orr, M.C., Wang, H., Zhang, A.B., 2022.
1 79 Identification of Species by Combining Molecular and Morphological Data Using
1 8 Convolutional Neural Networks. Systematic Biology 71, 690–705.
1 81 doi:10.1093/sysbio/syab076.
- 1 82 Ying, X., 2019. An Overview of Overfitting and its Solutions. Journal of Physics:
1 83 Conference Series 1168, 022022. doi:10.1088/1742-6596/1168/2/022022.
- 1 84 Zarrei, M., Talent, N., Kuzmina, M., Lee, J., Lund, J., Shipley, P.R., Stefanović, S.,
1 85 Dickinson, T.A., 2015. DNA barcodes from four loci provide poor resolution of
1 86 taxonomic groups in the genus *Crataegus*. AoB PLANTS 7, plv045.
1 87 doi:10.1093/aobpla/plv045.
- 1 88 Zhang, A.B., Sikes, D.S., Muster, C., Li, S.Q., 2008. Inferring Species Membership Using
1 89 DNA Sequences with Back-Propagation Neural Networks. Systematic Biology 57,
1 9 202–215. doi:10.1080/10635150802032982.
- 1 91 Zhang, D., Zhang, W., Zhao, Y., Zhang, J., He, B., Qin, C., Yao, J., 2023. DNAGPT: A
1 92 Generalized Pre-trained Tool for Versatile DNA Sequence Analysis Tasks.
1 93 doi:10.1101/2023.07.11.548628.